arXiv:1301.4798v1 [cs.IT] 21 Jan 2013

A Novel Mode Switching Scheme Utilizing Random Beamforming for Opportunistic Energy Harvesting

Hyungsik Ju and Rui Zhang

Abstract

Since radio signals carry both energy and information simultaneously, a unified study on simultaneous wireless information and power transfer (SWIPT) has recently attracted a great deal of attention for providing wireless energy to communication devices. This paper proposes a novel receiver mode switching scheme for SWIPT and the enabling transmitter design for a point-to-point multiple-input single-output (MISO) channel when the channel state information (CSI) is not available at the transmitter. The proposed scheme employs random beamforming at the transmitter to generate artificial channel fading to enable opportunistic energy harvesting at the receiver when the channel power exceeds a certain threshold. For the proposed scheme, we investigate the achievable average information rate, average harvested energy, and energy outage probability, as well as their various trade-offs in fading channels. Compared to a reference scheme of periodic receiver mode switching without random transmit beamforming, the proposed scheme is shown to be able to achieve better rate-energy trade-offs when the harvested energy target is sufficiently large. Particularly, it is revealed that employing one single random beam for the proposed scheme is asymptotically optimal as the transmit power increases to infinity, and also performs the best with finite transmit power for high energy harvesting requirements of practical interests, thus leading to an appealing low-complexity implementation. Finally, we compare the rate-energy performance of the proposed scheme with selected random beam designs.

Index Terms

Simultaneous wireless information and power transfer (SWIPT), wireless power, mode switching, multi-antenna system, random beamforming, rate-energy trade-off, energy outage.

I. INTRODUCTION

Conventionally, fixed energy supplies (e.g. batteries) are employed in energy-constrained wireless networks, such as sensor networks. The lifetime of the network is typically limited, and is thus one of the most important considerations for designing the network. To prolong the network's operation time, energy harvesting has recently attracted a great deal of attention since it enables scavenging energy from the environment and potentially provides unlimited power supplies for wireless networks.

Among other commonly used energy sources (e.g. solar and wind), radio signals radiated by ambient transmitters have drawn an upsurge of interest as a viable new source for wireless energy harvesting. Harvesting energy

The authors are with the Department of Electrical and Computer Engineering, National University of Singapore (e-mail: elejhs@nus.edu.sg, elezhang@nus.edu.sg).

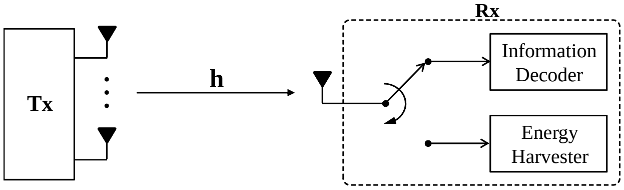

Fig. 1. A MISO wireless system for SWIPT via receiver mode switching.

from radio signals has already been successfully implemented in applications such as passive radio-frequency identification (RFID) systems and body sensor networks (BSNs) for medical implants. More interestingly, wireless energy harvesting opens an avenue for the joint investigation of simultaneous wireless information and power transfer (SWIPT) since radio signals carry energy and information at the same time. SWIPT has recently been investigated for various wireless channels, e.g., the point-to-point additive white Gaussian noise (AWGN) channel [1], [2], the frequency selective and/or fading channels [3], [4], the multi-antenna channels [5], [6], [7], and the multiple-access and relay channels [8].

To achieve optimal wireless energy transfer (WET) and wireless information transfer (WIT) simultaneously, one key challenge is to develop receiver architectures to enable information decoding (ID) and energy harvesting (EH) from the same received signal at the same time [2]. Practically, two suboptimal receiver designs for SWIPT have been proposed in [5] based on the principle of orthogonalizing ID and EH, namely *power splitting* and *time switching*. The power splitting scheme splits the received signal into two streams of different power for ID and EH separately, while the time switching scheme switches the receiver between an ID mode and an EH mode from time to time. The optimal switching rules between ID versus EH modes for a point-to-point single-antenna fading channel subject to the co-channel interference have been derived in [4] to maximize the average harvested energy given an information-rate target. It was shown in [4] that the time-fluctuation or fading of wireless channels is indeed beneficial for receiver mode-switching (time-switching) based SWIPT systems, where an “opportunistic” energy harvesting scheme is proved to be optimal, i.e., the receiver should switch to the EH mode when the channel power is larger than a certain threshold, and to the ID mode otherwise.

In this paper, we further investigate the receiver mode-switching based SWIPT in a point-to-point multiple-input single-output (MISO) system as shown in Fig. 1. It is assumed that the MISO channel from the transmitter to the receiver is quasi-static flat-fading, i.e., the channel remains constant during each block transmission, but varies from one block to another. It is also assumed that the MISO channel is perfectly known at the receiver in each block but unknown at the transmitter. Furthermore, we assume that the receiver has no given power supply and needs to replenish energy from the received signals via WET based on time-switching, i.e., the receiver can either decode information *or* harvest energy from the received signals at any time, but *not both*. In conventional wireless communication systems for WIT only, multi-antenna techniques have been widely applied to achieve spatial multiplexing [9] and/or spatial diversity [10], [11]. Furthermore, the use of multiple transmit antennas has been considered in wireless MISO broadcast channels to enable opportunistic communication by employing random transmit beamforming [12], [13], which generates artificial time-variations in quasi-static channels. In this paper, we apply the random beamforming technique in MISO point-to-point systems for a new usage, i.e., to enable opportunistic energy harvesting at the time-switching receiver for more efficient SWIPT implementation.

The main contributions of this paper are summarized as follows:

- We propose a novel receiver mode switching scheme for SWIPT based on random transmit beamforming. The proposed scheme employs random beamforming at the multi-antenna transmitter to generate artificial channel fading in each transmission block during which the physical MISO channel is assumed to be constant. This is to most efficiently utilize the time-switching receiver for optimizing the simultaneous WET and WIT performance. For the proposed scheme, we characterize the performance trade-offs between WET and WIT by investigating the achievable rate and harvested energy in each transmission block given a fixed MISO channel, assuming Gaussian distributed random beams.
- We extend our analysis for the constant MISO channel to quasi-static fading MISO channels. We investigate the achievable average information rate and average harvested energy over different transmission blocks, and characterize their asymptotic trade-offs when the transmit power goes to infinity. It is shown that employing one single random beam for the proposed scheme achieves the best rate-energy (R-E) trade-off in fading MISO channels asymptotically. Furthermore, we compare the R-E performance of our proposed scheme with that of a reference scheme with periodic switching between ID and EH modes, but without random transmit beamforming applied.
- When the receiver consumes significant amount of energy at each block and/or the capacity of its energy storage device is limited, the receiver may suffer from energy shortage unless the amount of harvested energy in each block is larger than a certain requirement. We thus study the “energy outage probability” of the proposed scheme in fading MISO channels, which is compared to the periodic switching in both asymptotic and finite transmit power regimes.
- In practice, transmit power is preferable to be constant for the optimal operation efficiency of transmitter amplifier. However, the use of Gaussian distributed random beams for the proposed scheme can cause large transmit power fluctuations. We thus propose alternative random beam designs with more stable transmit power,

for which the R-E performance is characterized and compared with the case of Gaussian random beam.

The rest of this paper is organized as follows. Section II introduces the proposed scheme, and derives the harvested energy and achievable information rate for a block of given MISO channel. Section III investigates the R-E performance for the proposed scheme in fading MISO channels. Section IV compares the performance of the proposed scheme with different random beam designs. Finally, Section V concludes the paper.

Notations: In this paper, matrices and vectors are denoted by bold-face upper-case letters and lower-case letters, respectively. $\mathbf{I}_N$ denotes an $N \times N$ identity matrix and $\mathbf{0}$ represents a matrix with all zero entries. The distribution of a circularly symmetric complex Gaussian (CSCG) random vector with mean vector $\boldsymbol{\mu}$ and covariance matrix $\boldsymbol{\Sigma}$ is denoted by $\mathcal{CN}(\boldsymbol{\mu}, \boldsymbol{\Sigma})$, and $\sim$ stands for "distributed as". $\mathbb{C}^{a\times b}$ and $\mathbb{R}^{a\times b}$ denote the spaces of $a \times b$ matrices with complex and real entries, respectively. $\|\mathbf{z}\|$ denotes the Euclidean norm of a complex vector $\mathbf{z}$. $\mathbb{E}\left[\cdot\right]$ represents the statistical expectation.

II. System Model

As shown in Fig. 1, this paper considers a point-to-point SWIPT system consisting of one transmitter (Tx) and one receiver (Rx). Tx is equipped with $N_t > 1$ antennas and Rx is equipped with one single antenna. It is assumed that the MISO channel from Tx to Rx follows quasi-static flat-fading, where the channel remains constant during each block transmission time, denoted by T, but varies from one block to another. It is further assumed that the channel is perfectly known at Rx, but is not known at Tx.

The transmitted signal at the nth symbol interval in one transmission block of interest is denoted by $\mathbf{x}\left(n\right) \in \mathbb{C}^{N_t\times 1}$. The covariance matrix of the transmitted signal is thus given by $\mathbf{S}_{\mathbf{x}} = \mathbb{E}[\mathbf{x}\left(n\right)\mathbf{x}^H\left(n\right)] = \frac{P}{N_t}\mathbf{I}_{N_t}$, where P denotes the total transmit power, which is assumed to be equally allocated among N_t transmit antennas. The received signal at Rx is then expressed as

$$y\left(n\right) = \mathbf{h}^T\mathbf{x}\left(n\right) + z\left(n\right), \tag{1}$$

where $y\left(n\right)$ and $z\left(n\right)$ denote the received signal and noise at Rx, respectively; and it is assumed that $z\left(n\right) \sim \mathcal{CN}\left(0,1\right)$ and is independent over n. The MISO channel from Tx to Rx is denoted by $\mathbf{h} \in \mathbb{C}^{N_t\times 1}$, which is constant during each transmission block.

In each block, Tx aims at achieving SWIPT to Rx. It is assumed that Rx is equipped with a rechargeable battery to store the energy harvested from the received signal, which is used to provide power to its operating circuits. Specifically, Rx harvests energy from the received signals when it is in the EH mode, while it decodes information in the ID mode. We assume that Rx switches between ID mode and EH mode as in [4], [5] since it is difficult yet

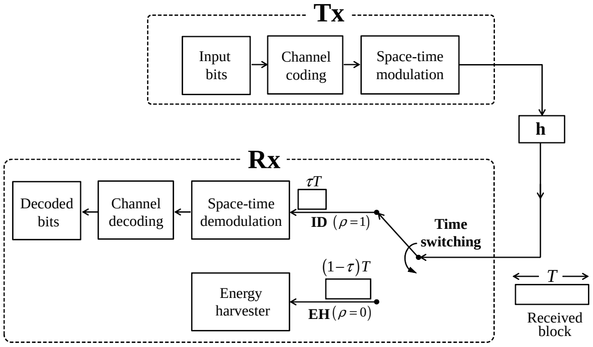

Fig. 2. Transmitter and receiver structures for periodic switching (PS).

to use the received signal for both ID and EH at the same time due to practical circuit limitations [2]. As in [4], ID mode and EH mode are represented by defining an indicator function as

$$\rho = \begin{cases} 1, & \text{ID mode is active} \\ 0, & \text{EH mode is active.} \end{cases} \tag{2}$$

We consider two time switching schemes, namely "*periodic switching* (PS)" and "*threshold switching* (TS)" as elaborated next.

A. Reference Scheme: Periodic Switching

As shown in Fig. 2, with PS Rx sets $\rho = 1$ during the first τT amount of time in each transmission block, with $0 \leq \tau \leq 1$, and $\rho = 0$ for the remaining block duration $(1-\tau)T$.[1] For given $\mathbf{h}$ and τ, the amount of harvested energy (normalized by T) in a transmission block can be derived using $\mathbf{S_x}$ as

$$\begin{aligned} E^{(\mathrm{P})}(H, \tau) &= (1-\tau)\,\zeta \mathbb{E}\left[\left\|\mathbf{h}^T \mathbf{x}(n)\right\|^2\right] \\ &= (1-\tau)\,\zeta P H, \end{aligned} \tag{3}$$

where $H = \frac{1}{N_t}\|\mathbf{h}\|^2$ is the average channel power per transmitting antenna, and $0 < \zeta \leq 1$ is a constant reflecting the loss in the energy transducer when the harvested energy is converted to electrical energy to be stored. In (3), it has been assumed that the energy harvested due to the receiver noise is negligible and thus is ignored. It is further assumed that $\zeta = 1$ in the sequel for notational brevity.

The transmitter structure for PS is also shown in Fig. 2. Note that with PS Rx can adjust τ based on its energy and rate requirements, as well as the channel condition. However, instead of requiring Rx to feed back the values of τ to Tx to maintain synchronized information transmission, which incurs additional overhead, Tx can employ the rateless code [14] for channel coding to realize a seamless information transmission to Rx regardless of τ.[2] The

[1] Ideally, with a given time allocation τ, setting $\rho = 1$ or 0 at the beginning of each block will not change the system performance; however, setting $\rho = 1$ initially may be practically more favorable for Rx to implement block-wise time synchronization.

[2] This is especially useful when the setup of this paper is extended to the case of multiple receivers in a wireless information-multicast channel, where receivers can set different values of τ for decoding common information sent by the transmitter, based on their channel conditions and energy requirements.

bit stream to be transmitted during a transmission block is thus first encoded by a rateless code. Space-time (ST) code is then applied to modulate the output bits from the rateless-code encoder, and the modulated symbols are transmitted by N_t antennas. We consider a ST code of length L, denoted by matrix $\mathbf{X}^{(\mathrm{P})} \in \mathbb{C}^{L \times N_t}$. It is assumed that $\mathbf{X}^{(\mathrm{P})}$ is a capacity-achieving ST code.[3]

Tx transmits a sequence of $\mathbf{X}^{(\mathrm{P})}$'s in each transmission block. Considering $\mathbf{X}^{(\mathrm{P})}$ with L consecutive transmitted symbols from each antenna, (1) is modified as

$$\mathbf{y} = \mathbf{X}^{(\mathrm{P})}\mathbf{h} + \mathbf{z}, \tag{4}$$

where $\mathbf{y} \in \mathbb{C}^{L \times 1}$ and $\mathbf{z} \in \mathbb{C}^{L \times 1}$ denote the received signal vector and noise vector, respectively, and $\mathbf{z} \sim \mathcal{CN}\left(\mathbf{0}, \mathbf{I}_L\right)$. Since $\mathbf{X}^{(\mathrm{P})}$ is assumed to be a capacity-achieving ST code, the achievable rate of the channel in (4) can be shown equivalent to that of a MISO channel $\mathbf{h}$ with input covariance matrix $\mathbf{S}_{\mathbf{x}} = \frac{P}{N_t}\mathbf{I}_{N_t}$. Assume that the number of ST coded blocks transmitted in each block is sufficiently large such that τT is approximately an integer number of the ST block durations for any value of τ. For given $\mathbf{h}$ and τ, the information rate for PS can thus be expressed as

$$R^{(\mathrm{P})}\left(H, \tau\right) = \tau \log_2\left(1 + PH\right). \tag{5}$$

Note that $R^{(\mathrm{P})}\left(H, \tau\right)$ is achievable when $N_t \leq 2$, but is in general an upper bound on the achievable rate when $N_t > 2$ for given $\mathbf{h}$ and τ.

B. Proposed Scheme: Threshold Switching

As shown in Fig. 3, the TS scheme is designed to take advantage of the received signal power fluctuations induced by transmit random beamforming within each transmission block for EH/ID mode switching, even with a constant MISO channel $\mathbf{h}$. For this purpose, each transmission block is further divided into K sub-blocks and artificial channel fading over different sub-blocks is generated by employing multi-antenna random beamforming at Tx.

Furthermore, at the kth sub-block, $k = 1, \ldots, K$, Rx determines whether to switch to ID mode or EH mode based on $A\left(k\right)$, which denotes the channel power at the kth sub-block (to be specified later). According to [4], in the presence of received channel power fluctuations, the optimal mode switching rule that achieves the optimal trade-off between the maximum harvested energy and information rate in a transmission block is given by

$$\rho\left(k\right) = \begin{cases} 1, & \text{if } A\left(k\right) \leq \bar{A} \\ 0, & \text{otherwise,} \end{cases} \tag{6}$$

---

[3] Alamouti code [10] is known as the capacity-achieving ST code when $N_t = 2$. For $N_t > 2$, capacity-achieving ST code has not yet been found in general. In this paper, however, capacity-achieving ST code is assumed even when $N_t > 2$ to provide a performance upper bound for the system under consideration.

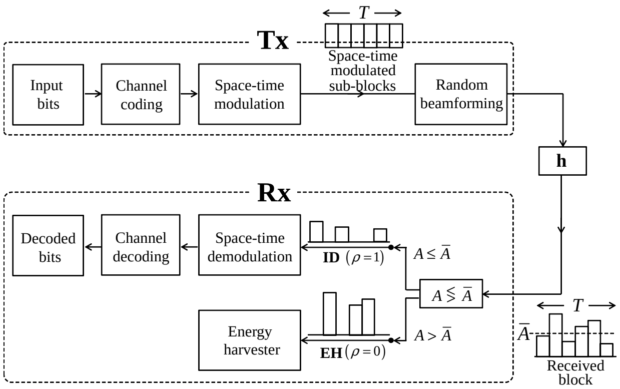

Fig. 3. Transmitter and receiver structures for threshold switching (TS).

where $\bar{A} \geq 0$ is a pre-designed threshold on the channel power. It is noted that choosing EH or ID mode at the kth sub-block is determined by the channel power $A\left(k\right)$, and the threshold on the corresponding *received signal power* thus increases linearly with P, which is given by $P\bar{A}$.

Artificial channel fading over sub-blocks is generated at Tx by using N random beams simultaneously, $1 \leq N \leq N_t$. Denote the nth random beam (RB) at the kth sub-block as $\boldsymbol{\phi}_n\left(k\right) \in \mathbb{C}^{N_t \times 1}$, where $\boldsymbol{\phi}_n\left(k\right) \sim \mathcal{CN}(\mathbf{0}, \frac{1}{N_t}\mathbf{I}_{N_t})$ assuming Gaussian RBs,[4] and $\mathbb{E}[\boldsymbol{\phi}_n\left(k\right)\boldsymbol{\phi}_m^H(j)] = \mathbf{0}$ if $k \neq j$ and/or $n \neq m$. Then it follows that $A\left(k\right) = \frac{1}{N}\left\|\mathbf{a}\left(k\right)\right\|^2$, where $\mathbf{a}\left(k\right) = \mathbf{\Phi}^T(k)\mathbf{h} \in \mathbb{C}^{N \times 1}$ is the equivalent MISO channel at the kth sub-block generated by $\mathbf{\Phi}\left(k\right) = [\boldsymbol{\phi}_1(k)\ \boldsymbol{\phi}_2(k)\ \cdots\ \boldsymbol{\phi}_N(k)]$. It can be easily verified that $\mathbf{a}\left(k\right) \sim \mathcal{CN}\left(\mathbf{0}, H\mathbf{I}_N\right)$ for a given H, and $A\left(k\right)$ is thus a chi-square random variable with $2N$ degrees-of-freedom. With N RBs and conditioned on a given MISO channel realization $\mathbf{h}$ with $H = h$, the probability density function (PDF) of $A := A\left(k\right)$, $\forall k$, and the cumulative distribution function (CDF) of A are given, respectively, as [15]

$$f_{A|H}^{(N)}\left(a\left|h\right.\right) = \frac{1}{\left(h/N\right)^N\Gamma\left(N\right)}a^{N-1}e^{-(N/h)a}, \tag{7}$$

$$F_{A|H}^{(N)}\left(a\left|h\right.\right) = 1 - \frac{\Gamma\left(N, \frac{Na}{h}\right)}{\Gamma\left(N\right)}, \tag{8}$$

where $\Gamma\left(x\right) = \int_0^\infty t^{x-1}e^{-t}dt$ and $\Gamma\left(\alpha, x\right) = \int_x^\infty t^{\alpha-1}e^{-t}dt$ represent the Gamma function and incomplete Gamma function, respectively. From (7) and (8), it can be inferred that the artificial channel fading induced by random transmit beamforming is more substantial over time with smaller N.

Similarly to PS, Tx with TS generates ST modulated symbols to be transmitted through the artificial fading MISO channels. However, they differ in two aspects. First, Tx with TS should employ the erasure code [16] instead of the rateless code in the case of PS. This is because the set of sub-blocks used for ID according to (6) are in general randomly distributed within a transmission block with $\bar{A} > 0$, and thus the resulting channel from Tx to Rx in ID mode can be modeled by an erasure channel for TS. Second, the ST code is applied over N RBs with TS instead of N_t antennas with PS. This is because the use of N RBs transforms the $N_t \times 1$ constant MISO channel $\mathbf{h}$ into an $N \times 1$ fading MISO channel specified by $\mathbf{a}\left(k\right)$'s in each transmission block. For each of the K sub-blocks in TS, we consider the use of a ST code of length L denoted by matrix $\mathbf{X}^{(\mathrm{T})} \in \mathbb{C}^{L \times N}$. For convenience, we express $\mathbf{X}^{(\mathrm{T})} = [\mathbf{x}_1^{(\mathrm{T})}\ \mathbf{x}_2^{(\mathrm{T})}\ \cdots\ \mathbf{x}_L^{(\mathrm{T})}]^T$, where $\mathbf{x}_l^{(\mathrm{T})} \in \mathbb{C}^{N \times 1}$, $1 \le l \le L$, denotes the lth transmitted signal vector in each ST coded block. The covariance matrix for $\mathbf{x}_l^{(\mathrm{T})}$ is given by $\mathbf{S}_{\mathbf{x},l}^{(\mathrm{T})} = \mathbb{E}[\mathbf{x}_l^{(\mathrm{T})}(\mathbf{x}_l^{(\mathrm{T})})^H] = \frac{P}{N}\mathbf{I}_N$, $\forall l$, to be consistent with $\mathbf{S}_{\mathbf{x}} = \frac{P}{N_t}\mathbf{I}_{N_t}$. Similar to $\mathbf{X}^{(\mathrm{P})}$ in the case of PS, $\mathbf{X}^{(\mathrm{T})}$ is assumed to be a capacity-achieving ST code for an equivalent MISO channel with N transmitting antennas.

---

[4] Alternative RB designs will be studied later in Section IV.

The received signal at each sub-block is used for either energy harvesting or information decoding according to (6). For the kth sub-block, the received signal can be expressed by modifying (1) as

$$\begin{aligned}\mathbf{y} &= \mathbf{X}^{(\mathrm{T})}\Phi^T\left(k\right)\mathbf{h} + \mathbf{z}\\ &= \mathbf{X}^{(\mathrm{T})}\mathbf{a}(k) + \mathbf{z},\end{aligned} \tag{9}$$

where $\mathbf{y} \in \mathbb{C}^{L \times 1}$ and $\mathbf{z} \in \mathbb{C}^{L \times 1}$ denote the received signal and noise vectors, respectively, with $\mathbf{z} \sim \mathcal{CN}\left(\mathbf{0}, \mathbf{I}_L\right)$. When $\rho\left(k\right) = 0$, the amount of harvested energy (normalized by sub-block duration T/K) at the kth sub-block is derived using $\mathbf{S}_{\mathbf{x},l}^{(\mathrm{T})}$ as

$$E^{(\mathrm{T})}\left(k\right) = \frac{1}{L}\mathbb{E}\left[\left\|\mathbf{X}^{(\mathrm{T})}\mathbf{a}(k)\right\|^2\right] = PA\left(k\right). \tag{10}$$

Furthermore, by assuming a capacity-achieving ST code, the achievable rate with TS at the kth sub-block when $\rho\left(k\right) = 1$ can be expressed as

$$R^{(\mathrm{T})}\left(k\right) = \log_2\left(1 + PA\left(k\right)\right). \tag{11}$$

The amount of harvested energy in a transmission block is the sum of the energy harvested from all sub-blocks in the EH mode. Assuming that $K \to \infty$, the harvested total energy (normalized by T) in a transmission block for given N RBs, threshold $\bar{A}$, and the realization of the MISO channel $\mathbf{h}$ with $H = h$ can be obtained from (10) as

$$\begin{aligned}E^{(\mathrm{T})}\left(h, N, \bar{A}\right) &= \frac{1}{T}\lim_{K\to\infty}\sum_{k=1}^{K}\left(1 - \rho\left(k\right)\right)\frac{T \times E^{(\mathrm{T})}\left(k\right)}{K}\\ &= \mathbb{E}\left[\left(1 - \rho\left(k\right)\right)PA\left(k\right)\right]\\ &= \int_{\bar{A}}^{\infty} Paf_{A|H}^{(N)}\left(a\left|h\right.\right)da \qquad (12)\\ &= Ph\frac{\Gamma\left(N+1, \frac{N\bar{A}}{h}\right)}{\Gamma\left(N+1\right)}, \qquad (13)\end{aligned}$$

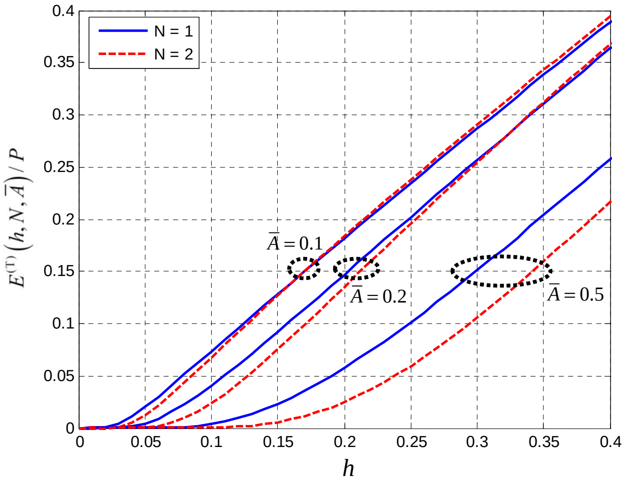

Fig. 4. $E^{(\mathrm{T})}\left(h,N,\bar{A}\right)/P$ vs. h with $N=1,2$ and $\bar{A}=0.1,\ 0.2,\ 0.5$.

where (13) can be obtained by applying (7) and [17, 3.351-2] to (12). From (13), it is observed that $E^{(\mathrm{T})}\left(h,N,\bar{A}\right)$ increases linearly with P. Thus, for a given P, the energy harvesting performance in a transmission block can be measured by the normalized harvested energy, $E^{(\mathrm{T})}\left(h,N,\bar{A}\right)/P$. Fig. 4 shows $E^{(\mathrm{T})}\left(h,N,\bar{A}\right)/P$ versus different values of h for $P=20$dB when $N=1,\ 2$ and $\bar{A}=0.1,\ 0.2,\ 0.5$. It is observed that $E^{(\mathrm{T})}\left(h,N,\bar{A}\right)/P$ decreases with increasing $\bar{A}$ when N and h are both fixed, which is in accordance with (13). Moreover, when N and $\bar{A}$ are both fixed, $E^{(\mathrm{T})}\left(h,N,\bar{A}\right)/P$ is observed to increase monotonically with h. This is because $F_{A|H}^{(N)}\left(\bar{A}\,|h\right)$ in (8) decreases with increasing h, and thus $1-F_{A|H}^{(N)}\left(\bar{A}\,|h\right)$, which is the percentage of the received sub-blocks allocated to EH mode in each block, increases. Thus, the amount of harvested energy in each block increases with h thanks to the increased number of sub-blocks assigned to EH mode, as well as the increased average channel power h, as can be inferred from (13).

Furthermore, when h and $\bar{A}$ are both fixed, $E^{(\mathrm{T})}\left(h,N,\bar{A}\right)/P$ is observed to decrease with increasing N when h is small, but increase with N when h is sufficiently large. This is because the artificial channel fading is more substantial when smaller number of RBs, N, is used, although the same average channel power is given as h. Given $1\leq N\leq N_t$, it can be shown that $F_{A|H}^{(N)}\left(\bar{A}\,|h\right)$ in (8) increases with N when h is small, and thus larger energy is harvested with smaller number of RBs. In contrast, it can also be shown that $F_{A|H}^{(N)}\left(\bar{A}\,|h\right)$ decreases with increasing N when h is larger than a certain threshold, and thus more energy is harvested with larger number of RBs. Similarly, we can verify that $E^{(\mathrm{T})}\left(h,N,\bar{A}\right)/P$ increases with N when $\bar{A}$ is small, but decreases with increasing N when $\bar{A}$ is sufficiently large.

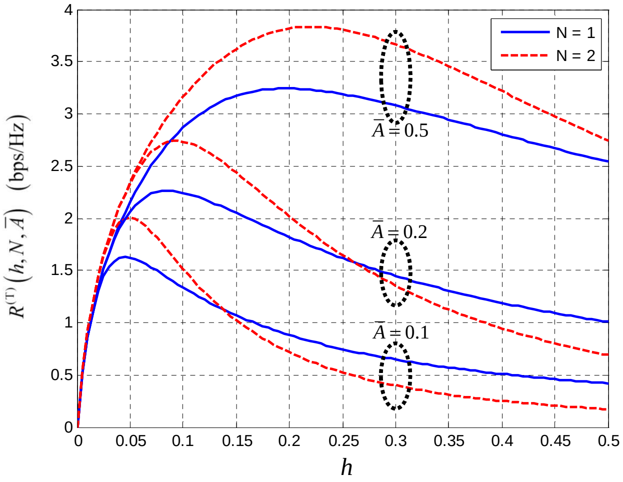

Fig. 5. $R^{(\mathrm{T})}\left(h, N, \bar{A}\right)$ vs. h with $P = 20$dB, $N = 1, 2$, and $\bar{A} = 0.1$, 0.2, 0.5.

Next, the achievable rate in a block for given N, $\bar{A}$, and h can be derived from (7) and (11) as

$$\begin{aligned} R^{(\mathrm{T})}\left(h, N, \bar{A}\right) &= \mathbb{E}\left[\rho\left(k\right)\log_2\left(1 + PA\left(k\right)\right)\right] \\ &= \int_0^{\bar{A}} \log_2\left(1 + Pa\right) f_{A|H}^{(N)}\left(a\left|h\right.\right) da. \end{aligned} \tag{14}$$

With $f_{A|H}^{(N)}\left(a\left|h\right.\right)$ given in (7), it is in general difficult to obtain a unified closed-form expression of (14) for arbitrary values of N. However, it is possible to derive closed-form expressions for (14) for some special values of N. For example, $R^{(\mathrm{T})}\left(h, 1, \bar{A}\right)$ and $R^{(\mathrm{T})}\left(h, 2, \bar{A}\right)$ for $N = 1$ and 2, respectively, are derived in closed-form in Appendix A. Fig. 5 shows $R^{(\mathrm{T})}\left(h, N, \bar{A}\right)$ versus different values of h for $P = 20$dB when $N = 1$, 2 and $\bar{A} = 0.1$, 0.2, 0.5. It is observed that $R^{(\mathrm{T})}\left(h, N, \bar{A}\right)$ increases with $\bar{A}$ when N and h are both fixed, which is in accordance with (14). Moreover, by the opposite argument of the explanation for Fig. 4, when h and $\bar{A}$ are both fixed, $R^{(\mathrm{T})}\left(h, N, \bar{A}\right)$ is observed to increase with N when h is small or $\bar{A}$ is large, but decrease with increasing N when h or $\bar{A}$ is sufficiently large/small.

However, different from $E^{(\mathrm{T})}\left(h, N, \bar{A}\right)/P$ in Fig. 4 which is a monotonically increasing function of h, it is observed in Fig. 5 that $R^{(\mathrm{T})}\left(h, N, \bar{A}\right)$ in general first increases with h, and then decreases with increasing h for given N and $\bar{A}$. The reason is as follows. When $h \to 0$, from (14), we have $R^{(\mathrm{T})}\left(h, N, \bar{A}\right) \to \log_2\left(1 + Ph\right)$; thus, $R^{(\mathrm{T})}\left(h, N, \bar{A}\right)$ increases with h. However, when $h \to \infty$, $f_{A|H}^{(N)}\left(\bar{A}\left|h\right.\right) \to 0$ for any finite $0 \le a \le \bar{A}$, and thus $R^{(\mathrm{T})}\left(h, N, \bar{A}\right) \to 0$; therefore, $R^{(\mathrm{T})}\left(h, N, \bar{A}\right)$ should decrease with increasing h when h is sufficiently large.

C. Rate-Energy Performance Comparison

As in [4] and [5], there exist rate-energy (R-E) trade-offs in both PS and TS for information and energy transfer. R-E trade-offs in PS and TS can be characterized by setting different values of τ and $\bar{A}$, respectively. Fig. 6 shows

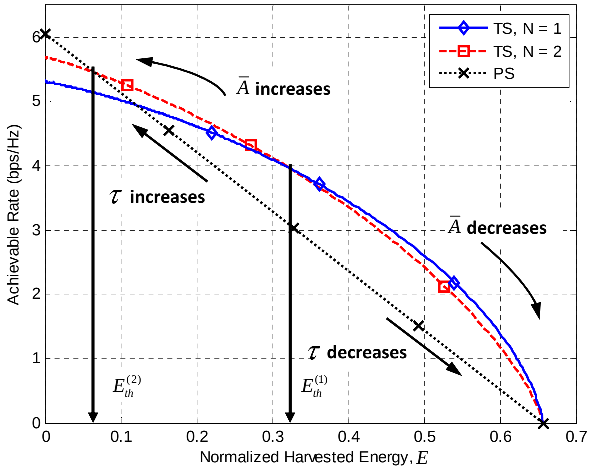

Fig. 6. Trade-offs between achievable rate and harvested energy when $P = 20\text{dB}$, $N_t = 2$, and $\mathbf{h} = [1.0 \;\; 0.56]^T$.

R-E trade-offs in PS and TS for $N_t = 2$ and a constant MISO channel $\mathbf{h} = [1.0 \;\; 0.56]^T$. For PS, $\mathbf{X}^{(\mathrm{P})}$ is generated by Alamouti code with $L = 2$ [10]. For TS, a scalar code cascaded by one single RB is applied when $N = 1$, while the Alamouti code with two RBs is applied when $N = 2$. The harvested energy normalized by P is denoted by E. It is observed that TS yields the best R-E trade-off with $N = 1$ when $E_{th}^{(1)} \leq E \leq h$, and with $N = 2$ when $E_{th}^{(2)} \leq E < E_{th}^{(1)}$, while PS yields the best R-E trade-off when $0 \leq E < E_{th}^{(2)}$, where $E_{th}^{(1)}$ and $E_{th}^{(2)}$ are shown in Fig. 6. Note that at $E = 0$, i.e., no EH is required as in the conventional MISO system with WIT only, PS achieves higher rate than TS since artificial channel fading by random beamforming degrades the AWGN channel capacity. However, when the harvested energy exceeds certain thresholds, i.e., $E_{th}^{(2)}$ and $E_{th}^{(1)}$, TS with $N = 2$ RBs and $N = 1$ RB achieves the best rate performance for a given energy target, respectively. This demonstrates the unique usefulness of random beamforming in a multi-antenna SWIPT system even with constant channels.

It is worth noting that for TS larger information rate is achieved with $N = 1$ when $E_{th}^{(1)} \leq E \leq h$, but with $N = 2$ otherwise. This can be explained as follows. For a given h, it can be shown from (13) that $\bar{A} \to 0$ when $E \to h$. Thus, with sufficiently small $\bar{A}$, we have $E^{(\mathrm{T})}\left(h, 1, \bar{A}\right) \approx E^{(\mathrm{T})}\left(h, 2, \bar{A}\right)$ (note that $E^{(\mathrm{T})}\left(h, 2, \bar{A}\right)$ is sightly larger than $E^{(\mathrm{T})}\left(h, 1, \bar{A}\right)$ for small $\bar{A}$ as discussed for Fig. 4; but the gap between them is negligible as shown in Fig. 4 with $\bar{A} = 0.1$). On the other hand, with small $\bar{A}$, it can be shown from (7) that $f_{A|H}^{(1)}\left(a\,|h\right) > f_{A|H}^{(2)}\left(a\,|h\right)$, $0 \leq a \leq \bar{A}$, and thus $R^{(\mathrm{T})}\left(h, 1, \bar{A}\right) > R^{(\mathrm{T})}\left(h, 2, \bar{A}\right)$ from (14), as discussed for Fig. 5. Therefore, TS with $N = 1$ achieves larger information rate than $N = 2$ when E is sufficiently large. In contrast, as $E \to 0$, we have $\bar{A} \to \infty$ from (13). Then, it can be shown that $R^{(\mathrm{T})}\left(h, 1, \infty\right) < R^{(\mathrm{T})}\left(h, 2, \infty\right)$ since the ergodic capacity of a fading MISO channel increases with the number of transmit antennas. Therefore, for TS larger information rate is achieved with $N = 2$ than $N = 1$ when E is smaller than a certain threshold.

III. PERFORMANCE ANALYSIS IN FADING CHANNEL

In this section, the R-E performances of TS and PS schemes are analyzed in MISO fading channels. It is assumed that the MISO channel is independent and identically distributed (i.i.d.) Rayleigh fading channel with $\mathbf{h} \sim \mathcal{CN}\left(\mathbf{0}, \mathbf{I}_{N_t}\right)$, and thus $H = \frac{1}{N_t}\|\mathbf{h}\|^2$ is a chi-square random variable with $2N_t$ degrees-of-freedom, with the following PDF and CDF [15]:

$$f_H\left(h\right) = \frac{{N_t}^{N_t}}{\Gamma\left(N_t\right)} h^{N_t-1} e^{-N_t h}, \tag{15}$$

$$F_H\left(h\right) = 1 - \frac{\Gamma\left(N_t, N_t h\right)}{\Gamma\left(N_t\right)}. \tag{16}$$

In practice, it is possible for Rx to change $\bar{A}$ for TS or τ for PS with the fading MISO channel $\mathbf{h}$ for different transmission blocks; however, this incurs additional complexity at Rx. In this section, for simplicity, it is assumed that $\bar{A}$ and τ are set to be fixed values over different realizations of $\mathbf{h}$.

A. Achievable Average Information Rate

We consider that the performance of information transfer is measured by the achievable average rate over fading channels. Given N and $\bar{A}$, the achievable average rate of TS is denoted by $\bar{R}^{(\mathrm{T})}\left(N, \bar{A}\right) = \mathbb{E}_H\left[R^{(\mathrm{T})}\left(h, N, \bar{A}\right)\right]$, where $R^{(\mathrm{T})}\left(h, N, \bar{A}\right)$ is given by (14) for a given h. However, it is difficult to obtain the closed-form expressions for $\bar{R}^{(\mathrm{T})}\left(N, \bar{A}\right)$'s using (14) and (15) for any given N, $1 \leq N \leq N_t$.

Note that in practice, SWIPT systems usually operate with large transmit power P due to the requirement of energy transfer. Therefore, as P is sufficiently large, $R^{(\mathrm{T})}\left(h, N, \bar{A}\right)$ in (14) can be approximated as

$$R^{(\mathrm{T})}\left(h, N, \bar{A}\right) \approx F_{A|H}^{(N)}\left(\bar{A}\left|h\right.\right) \log_2\left(P\right) + C_0\left(h, N, \bar{A}\right), \tag{17}$$

where $F_{A|H}\left(\bar{A}\left|h\right.\right) = \int_0^{\bar{A}} f_{A|H}\left(a\left|h\right.\right) da$ and $C_0\left(h, N, \bar{A}\right) = \int_0^{\bar{A}} \log_2\left(a\right) f_{A|H}\left(a\left|h\right.\right) da$, which is a constant not related to P. Fig. 7 shows $R^{(\mathrm{T})}\left(h, N, \bar{A}\right)$ and its approximation by (17) versus P with $N = 1$ for different values of h and $\bar{A}$. It is observed that the approximation in (17) is more accurate as h and/or $\bar{A}$ increases. It is also observed that the gap between the achievable rate and its approximation becomes negligible when $P \geq 30$dB even with small values of $h = 0.1$ and $\bar{A} = 0.05$.

With the approximation of $R^{(\mathrm{T})}\left(h, N, \bar{A}\right)$ by (17), we can characterize the asymptotic behavior of $\bar{R}^{(\mathrm{T})}\left(N, \bar{A}\right)$ as P becomes large by investigating its pre-log scaling factor, which is given by the following proposition.

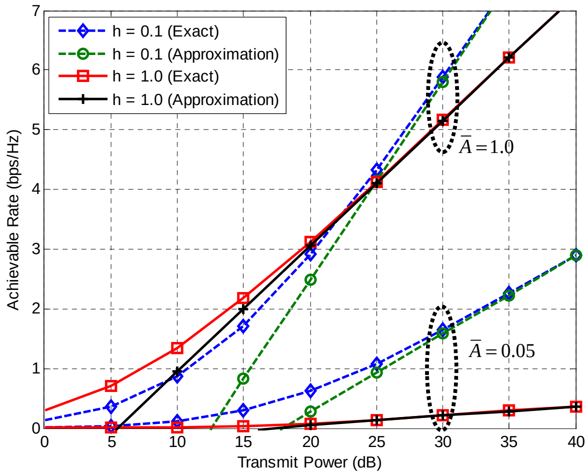

Fig. 7. Plot of $R^{(\mathrm{T})}\left(h, N, \bar{A}\right)$ with $N = 1$, $h = 0.1$ and 1.0, $\bar{A} = 0.05$ and 1.0.

Proposition 3.1: Given $1 \leq N \leq N_t$ and $\bar{A} \geq 0$, the achievable average rate for TS over the i.i.d. Rayleigh fading MISO channel is obtained as $\bar{R}^{(\mathrm{T})}\left(N, \bar{A}\right) = \Delta^{(\mathrm{T})}\left(N, \bar{A}\right) \log_2(P) + o\left(\log_2 P\right)$ with $P \to \infty$, where[5]

$$\Delta^{(\mathrm{T})}\left(N, \bar{A}\right) \triangleq \lim_{P \to \infty} \frac{\bar{R}^{(\mathrm{T})}\left(N, \bar{A}\right)}{\log_2 P} = F_A^{(N)}\left(\bar{A}\right), \tag{18}$$

with $F_A^{(N)}(a) = \mathbb{E}_H\left[F_{A|H}^{(N)}\left(a\,|h\right)\right]$ denoting the unconditional CDF of A after averaging over the fading distribution, which can be further expressed as

$$F_A^{(N)}(a) = 1 - \frac{2}{\Gamma\left(N_t\right)} \sum_{k=0}^{N-1} \frac{\beta^{N_t+k}}{k!} K_{N_t-k}\left(2\beta\right), \tag{19}$$

where $\beta = \sqrt{N_t N a}$, and $K_\delta(x)$ denotes the second-kind modified Bessel function

$$K_\delta(x) = \frac{\pi}{2} \frac{I_{-\delta}(x) - I_\delta(x)}{\sin(\delta x)},$$

with $I_\delta(x)$ denoting the first-kind modified Bessel function

$$I_\delta(x) = \sum_{m=0}^{\infty} \frac{1}{m!\,\Gamma(m + \delta + 1)} \left(\frac{x}{2}\right)^{2m+\alpha}.$$

Proof: Please refer to Appendix B. ■

Remark 3.1: In the fading MISO channel, $F_A^{(N)}\left(\bar{A}\right)$ denotes the percentage of sub-blocks allocated to ID mode for TS. From Proposition 3.1, it is inferred that $F_A^{(N)}\left(\bar{A}\right)$ is also the pre-log rate scaling factor of the asymptotic achievable average information rate over the MISO fading channel for TS with given $\bar{A}$ and N.

Fig. 8 shows $F_A^{(N)}\left(\bar{A}\right)$ versus $\bar{A}$ for TS with $N_t = 4$ in the i.i.d. Rayleigh fading MISO channel. From Fig. 8, it is observed that the rate scaling factor $F_A^{(N)}\left(\bar{A}\right)$ for TS increases with decreasing N when $\bar{A}$ is small, but

---

[5] $f(x) = o\left(g(x)\right)$ as $x \to x_0$ represents that $\lim_{x \to x_0} \frac{f(x)}{g(x)} = 0$, meaning intuitively that $f(x) \ll g(x)$ as $x \to x_0$.

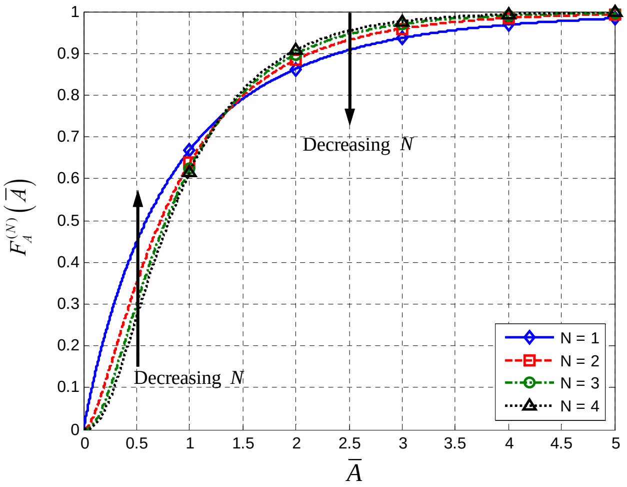

Fig. 8. $F_A^{(N)}\left(\bar{A}\right)$ vs. $\bar{A}$ when $N_t = 4$.

decreases with N when $\bar{A}$ is sufficiently large. As a result, $\bar{R}^{(\mathrm{T})}\left(N, \bar{A}\right)$ scales faster with increasing P for smaller value of N when $\bar{A}$ is small, but scales slower with P when $\bar{A}$ becomes large.

On the other hand, the rate scaling factor for PS in the i.i.d. Rayleigh fading MISO channel can be determined from (5) and (15) as

$$\Delta^{(\mathrm{P})}\left(\tau\right) = \lim_{P\rightarrow\infty} \frac{\mathbb{E}_H\left[R^{(\mathrm{P})}\left(h,\tau\right)\right]}{\log_2 P} = \tau. \tag{20}$$

B. *Average Harvested Energy*

In this subsection, we study the average harvested energy over the i.i.d. Rayleigh fading MISO channel by TS, defined as $\bar{E}^{(\mathrm{T})}\left(N, \bar{A}\right) = \mathbb{E}_H\left[E^{(\mathrm{T})}\left(h, N, \bar{A}\right)\right]$, where $E^{(\mathrm{T})}\left(h, N, \bar{A}\right)$ is given by (13).

Proposition 3.2: In the i.i.d. Rayleigh fading MISO channel, for given $\bar{A}$ and N, the average harvested energy for TS is given by

$$\bar{E}^{(\mathrm{T})}\left(N, \bar{A}\right) = P\frac{2}{\Gamma\left(N_t\right)} \sum_{k=0}^{N} \frac{\beta^{N_t+k}}{k!} \sqrt{\frac{N\bar{A}}{N_t}} K_{N_t-k+1}\left(2\beta\right), \tag{21}$$

where β and $K_\delta\left(x\right)$ are defined in Proposition 3.1.

Proof: Please refer to Appendix C. ■

For convenience, we term $\Pi^{(\mathrm{T})}\left(N, \bar{A}\right) = E^{(\mathrm{T})}\left(N, \bar{A}\right)/P$ as the *energy scaling factor* for TS with increasing P. Fig. 9 shows $\Pi^{(\mathrm{T})}\left(N, \bar{A}\right)$ versus different values of $\bar{A}$ with $N_t = 4$. It is observed that the energy scaling factor $\Pi^{(\mathrm{T})}\left(N, \bar{A}\right)$ for TS behaves in the opposite way of the rate scaling factor $F_A^{(N)}\left(\bar{A}\right)$, as compared to Fig. 8, i.e., $\Pi^{(\mathrm{T})}\left(N, \bar{A}\right)$ decreases with N when $\bar{A}$ is small, but increases with decreasing N when $\bar{A}$ is sufficiently large. As a result, for a given P, $\bar{E}^{(\mathrm{T})}\left(N, \bar{A}\right)$ behaves the same as $\Pi^{(\mathrm{T})}\left(N, \bar{A}\right)$.

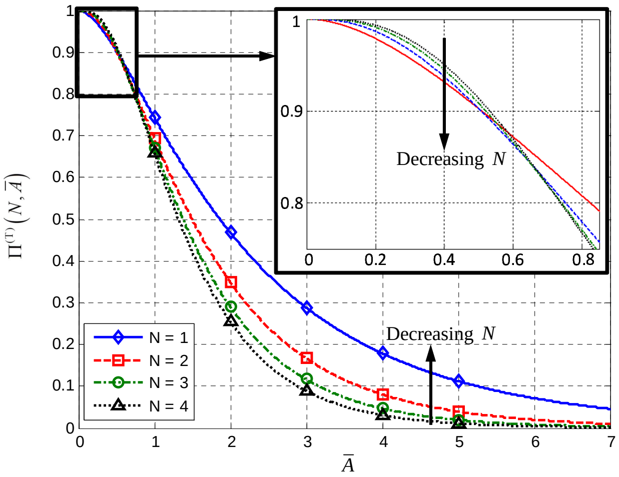

Fig. 9. $\Pi^{(\mathrm{T})}\left(N,\bar{A}\right)$ vs. $\bar{A}$ when $N_t = 4$.

On the other hand, the energy scaling factor for PS in the i.i.d. Rayleigh fading MISO channel can be easily obtained from (3) and (15) as

$$\Pi^{(\mathrm{P})}\left(\tau\right) = \mathbb{E}_H\left[E^{(\mathrm{P})}\left(h,\tau\right)\right]/P = \left(1-\tau\right), \ \ 0 \le \tau \le 1. \tag{22}$$

The rate and energy scaling factors characterize the asymptotic rate-energy trade-off as $P \to \infty$. Given $1 \le N \le N_t$, for TS it is easily shown from (19) and (21) that the rate scaling factor $\Delta^{(\mathrm{T})}\left(N,0\right) = 0$ and the energy scaling factor $\Pi^{(\mathrm{T})}(N,0) = 1$ at $\bar{A} = 0$, while $\Delta^{(\mathrm{T})}\left(N,\infty\right) = 1$ and $\Pi^{(\mathrm{T})}(N,\infty) = 0$ at $\bar{A} \to \infty$. Note that for TS the distribution of the received channel power $A\left(k\right)$ at each sub-block becomes different according to N, and as a result different asymptotic rate-energy trade-off is achieved when $0 < \Delta^{(\mathrm{T})}\left(N,\bar{A}\right) < 1$ and $0 < \Pi^{(\mathrm{T})}\left(N,\bar{A}\right) < 1$. To characterize this trade-off, we have the following theorem.

Theorem 3.1: In the i.i.d. Rayleigh fading MISO channel, given $1 \le N \le N_t$ and $0 < \bar{A} < \infty$ for TS scheme and $0 < \tau < 1$ for PS scheme, $\Delta^{(\mathrm{T})}\left(N,\bar{A}\right) > \Delta^{(\mathrm{P})}\left(\tau\right)$ for a given energy scaling factor $0 < \Pi^{(\mathrm{T})}\left(N,\bar{A}\right) = \Pi^{(\mathrm{P})}\left(\tau\right) < 1$; furthermore, given $1 \le N < M \le N_t$ and $0 < \bar{A}_N, \bar{A}_M < \infty$ for TS schemes, $\Delta^{(\mathrm{T})}\left(N,\bar{A}_N\right) > \Delta^{(\mathrm{T})}\left(M,\bar{A}_M\right)$ for a given energy scaling factor $0 < \Pi^{(\mathrm{T})}\left(N,\bar{A}_N\right) = \Delta^{(\mathrm{T})}\left(M,\bar{A}_M\right) < 1$.

Proof: Please refer to Appendix D. ■

Fig. 10 shows the rate scaling factor ($\Delta^{(\mathrm{T})}\left(N,\bar{A}\right)$ for TS and $\Delta^{(\mathrm{P})}\left(\tau\right)$ for PS) versus energy scaling factor ($\Pi^{(\mathrm{T})}\left(N,\bar{A}\right)$ for TS and $\Pi^{(\mathrm{P})}\left(\tau\right)$ for PS) with $N_t = 4$. For a given $0 < \Pi^{(\mathrm{T})}\left(N,\bar{A}\right) = \Pi^{(\mathrm{P})}\left(\tau\right) < 1$, the rate scaling factor of TS with $N = 1$, i.e., one single random beam, is the largest among all values of N. In addition, $\Delta^{(\mathrm{T})}\left(N,\bar{A}\right)$ for TS decreases with increasing N, but is always larger than $\Delta^{(\mathrm{P})}\left(\tau\right)$ for PS. The above observatios are in accordance with Theorem 3.1.

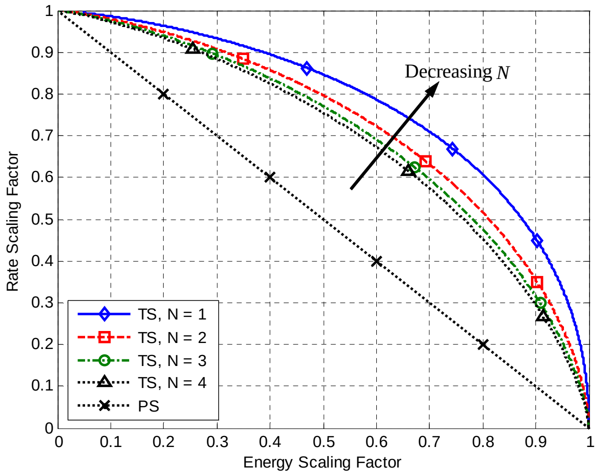

Fig. 10. Rate vs. energy scaling factors with $N_t = 4$.

C. Energy Outage Probability

In this subsection, we study the energy outage probability with a given harvested energy target $\hat{E}$ at Rx, which is defined as $p_{E,\,out} \overset{\Delta}{=} \Pr\left(E < \hat{E}\right)$ with E denoting the harvested energy in one block. In particular, we are interested in characterizing the asymptotic behavior of $p_{E,\,out}$ as $P \to \infty$, namely *energy diversity order*, which is defined as

$$d_E \overset{\Delta}{=} - \lim_{P\to\infty} \frac{\log p_{E,\,out}}{\log P}. \tag{23}$$

Proposition 3.3: In the i.i.d. Rayleigh fading MISO channel, for TS the energy outage probability $p^{(\mathrm{T})}_{E,out}$ with $P \to \infty$ is given by

$$p^{(\mathrm{T})}_{E,out} = \begin{cases} \left(\frac{\hat{E}}{P}\right)^{N_t} & , \ \bar{A} = 0 \\ \left(N\bar{A}(\ln P)^{-1}\right)^{N_t} & , \ \bar{A} > 0. \end{cases} \tag{24}$$

Proof: Please refer to Appendix G. ■

From (23) and (24), it can be verified that the energy diversity order of TS is $d^{(\mathrm{T})}_E = N_t$ when $\bar{A} = 0$, i.e., no WIT is required, and $d^{(\mathrm{T})}_E = 0$ with a fixed $\bar{A} > 0$ when both WIT and WET are implemented.

On the other hand, in the i.i.d. Rayleigh fading MISO channels, the energy outage probability of PS with $P \to \infty$ can be obtained as $p^{(\mathrm{P})}_{E,out} = \left(\frac{\hat{E}}{(1-\tau)P}\right)^{N_t}$, $0 \le \tau < 1$; thus, from (3) and the fact that $F_H(h) \approx h^{N_t}$ as $h \to 0$, we obtain the energy diversity order as $d^{(\mathrm{P})}_E = N_t$, $0 \le \tau < 1$.

Fig. 11 shows the energy outage probabilities of TS and PS versus P when $N_t = 2$ and $\hat{E} = 10$.[6] It is observed that the smallest energy outage probabilities are achieved by TS with $\bar{A} = 0$ or equivalently PS with $\tau = 0$. When $\bar{A} > 0$, $p^{(\mathrm{T})}_{E,out}$ for TS is observed to decrease slower with increasing P than $p^{(\mathrm{P})}_{E,out}$ for PS, since $d^{(\mathrm{T})}_E = 0$, $\bar{A} > 0$

---

[6] Here, one unit of energy represents the amount of harvested energy in one transmission block when $\bar{A} = 0$, $P = 1$, and $h = 1$.

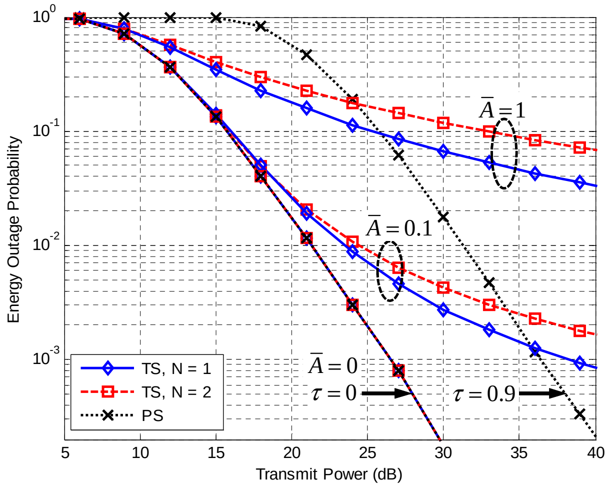

Fig. 11. Energy outage probability with $N_t = 2$ and $\hat{E} = 10$.

for TS while $d_E^{(\mathrm{P})} = N_t$, $0 \leq \tau < 1$, for PS. Furthermore, it is also observed that $p_{E,out}^{(\mathrm{T})}$ decreases slower with increasing P as $\bar{A}$ and/or N increases, which is consistent with (24).

D. Numerical Results

As inferred from Theorem 3.1, the asymptotic rate scaling factor of TS with $N = 1$ is the largest among all values of N and is also larger than that for PS for a given energy scaling factor as $P \to \infty$. However, it does not imply that the largest achievable average rate is always attained for a given average harvested energy when P is finite. Therefore, it is necessary to compare the achievable average rates for PS and TS with finite values of P. Fig. 12 shows the achievable average rates for PS and TS versus P under the same average energy harvesting requirement $\bar{E}$ ($\bar{E} = \bar{E}^{(\mathrm{T})}\left(N, \bar{A}\right)/P = \bar{E}^{(\mathrm{P})}\left(\tau\right)/P$) with $N_t = 2$. When $\bar{E} = 0.9$, the benefit from a larger rate scaling factor is clearly observed for TS with $N = 1$, since it achieves the largest average information rate. When $\bar{E} = 0.5$, the achievable average rates for TS are similar with $N = 1$ and 2, but still grow faster with P than that for PS. When $\bar{E} = 0.1$, the gaps between rate scaling factors of different schemes are small (c.f. Fig. 10) and as a result their achievable average rates become similar.

Next, Fig. 13 shows the trade-offs between the achievable average rate and energy non-outage probabilities, i.e., $1 - p_{E,out}$, of TS and PS schemes under the same per-block harvested energy requirement $\hat{E}$ with $P = 20$dB and $N_t = 2$. When $\hat{E} = 10$, it is observed that the energy non-outage (outage) probability of PS is the largest (smallest) for a given achievable average rate. However, when $\hat{E} = 50$, it is observed that the minimum energy outage probability of TS is attained by $N = 1$ when the achievable average rate is small, but by $N = 2$ when the achievable average rate is larger, while TS with both $N = 1$ and 2 outperforms PS.

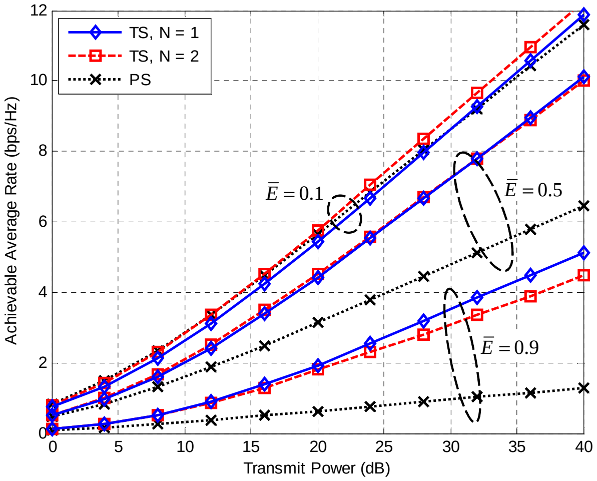

Fig. 12. Comparison of the achievable average rate with $N_t = 2$ and the average harvested energy requirement $\bar{E} = 0.1, 0.5$, and 0.9.

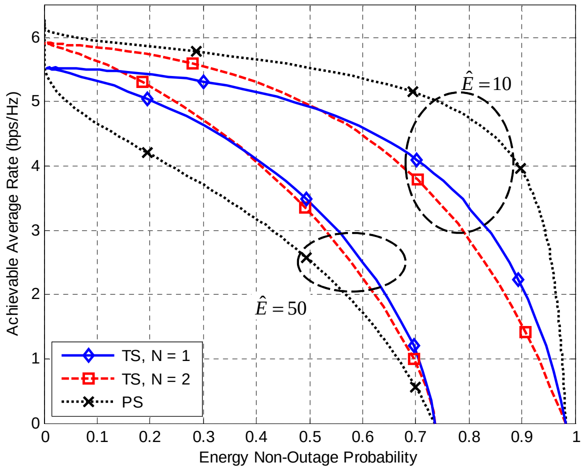

Fig. 13. Trade-off between achievable average rate and energy non-outage probability with $P = 20$dB, $N_t = 2$, and per-block harvested energy requirement $\hat{E} = 10$ and 50.

Remark 3.2: Employing random beamforming at the transmitter requires additional complexity. However, from the above results, it is inferred that the achievable average rate is maximized by using only one single RB, i.e., $N = 1$, when P is asymptotically large or at finite P when more harvested energy is required (which is of more practical interest). In addition, TS with one single RB also optimizes energy outage performance when P is finite and large harvested energy is required in each transmission block. Therefore, TS with one single RB can achieve the optimal WET efficiency and/or reliability with a given WIT rate requirement, thus yielding an appealing low-complexity implementation for practical systems.

IV. ALTERNATIVE RANDOM BEAM DESIGNS

It is worth noting that TS with Gaussian random beams (referred to as TS-G), as considered in the preceding sections, may not be practically favorable due to the fact that Gaussian random beams (GRBs) will cause infinite transmit power at certain sub-blocks. Instead, artificial channel fading within each transmission block can be generated by employing non-Gaussian random beams with constant transmit power for TS. In this section, we investigate the performance of TS with two alternative RBs other than GRB, such that the average transmit power remains constant within each transmission block, which are given next.

A. *Unitary Random Beams (URBs)*

In this case, N unitary random vectors obtained from the isotropic distribution [18] are independently employed for the N random beams at the kth sub-block, i.e., $\boldsymbol{\phi}_n(k)$, $1 \leq n \leq N$, $\forall k$.

With URBs, it is in general difficult to obtain the closed-form expressions for the PDF and CDF of the received channel power $A(k)$ at each sub-block conditioned on $H = h$. However, if we consider the special case of $N_t = 2$ and $N = 1$, it is known that with URBs $A(k)$ is uniformly distributed within $[0, 2h]$. Thus, given a threshold $\bar{A} \geq 0$, the amount of harvested energy in each block with URBs can be obtained using (12) as

$$E^{(\mathrm{U})}\left(h, \bar{A}\right) = \begin{cases} P(h - \frac{\bar{A}^2}{4h}) & , \quad 0 \leq \bar{A} \leq 2h \\ 0 & , \quad \bar{A} > 2h. \end{cases} \tag{25}$$

In the i.i.d. fading MISO channel, the average harvested energy for TS with URBs (referred to as TS-U) given a fixed threshold $\bar{A} \geq 0$ is obtained as $\bar{E}^{(\mathrm{U})}\left(\bar{A}\right) = \int_0^\infty E^{(\mathrm{U})}\left(h, \bar{A}\right) f_H(h)\, dh$, where $f_H(h) = 4he^{-2h}$ is given by (15) for $N_t = 2$. It is worth noting that in the special case of $N_t = 2$ and $N = 1$, the unconditional distribution of $A(k)$ with URBs after averaging over the fading channels can be shown to be the exponential distribution, where the unconditional PDF is given by $q_A^{(\mathrm{U})}(a) = e^{-a}$. Therefore, $\bar{E}^{(\mathrm{U})}\left(\bar{A}\right)$ can be alternatively obtained as

$$\begin{aligned} \bar{E}^{(\mathrm{U})}\left(\bar{A}\right) &= \int_{\bar{A}}^\infty P a q_A^{(\mathrm{U})}(a)\, da \\ &= P\Gamma\left(2, \bar{A}\right), \end{aligned} \tag{26}$$

which is equivalent to $E^{(\mathrm{T})}\left(1, 1, \bar{A}\right)$ for TS-G given by (13) with $N = 1$ and $h = 1$. Similarly, given $\bar{A} \geq 0$, the achievable average transmission rate for TS-U is obtained as

$$\begin{aligned} \bar{R}^{(\mathrm{U})}\left(\bar{A}\right) &= \int_0^{\bar{A}} \log_2(1 + Pa)\, q_A^{(\mathrm{U})}(a)\, da \\ &= \frac{e^{-\frac{1}{P}}}{\ln 2}\left(E_1\left(\frac{1}{P}\right) - E_1\left(\frac{1 + P\bar{A}}{P}\right)\right) - e^{-\bar{A}} \log_2\left(1 + P\bar{A}\right), \end{aligned} \tag{27}$$

which is also equivalent to $R^{(\mathrm{T})}\left(1,1,\bar{A}\right)$ for TS-G given by (14) with $h=1$ and $N=1$. In addition, given fixed $\bar{A}\geq 0$ and per-block energy harvesting requirement $\hat{E}>0$, the energy outage probability of TS-U in the i.i.d. Rayleigh fading MISO channel with $N_t=2$ and $N=1$ can be obtained from (25) as

$$p_{E,out}^{(\mathrm{U})}=F_H\left(\frac{\hat{E}^2+\sqrt{\hat{E}^2+\bar{A}^2P^2}}{2P}\right), \tag{28}$$

where $F_H\left(h\right)$ is given by (16) for $N_t=2$. From (23) and (28), it is easily verified that TS-U in the case of $N_t=2$ and $N=1$ has the energy diversity order of 0, the same as TS-G.

B. Binary Random Beams (BRBs)

In this case, a random subset of N out of N_t transmit antennas at Tx, $1\leq N\leq N_t$, are selected to transmit at each sub-block, which is equivalent to selecting $\mathbf{\Phi}\left(k\right)=\left[\boldsymbol{\phi}_1(k)\ \boldsymbol{\phi}_2(k)\ \cdots\ \boldsymbol{\phi}_N(k)\right]\in\mathbb{R}^{N_t\times N}$, $\forall k$, where $\boldsymbol{\phi}_n(k)=\left[\phi_{n,1}\left(k\right)\ \ \phi_{n,2}\left(k\right)\ \ \cdots\phi_{n,N_t}\left(k\right)\right]^T$, $1\leq n\leq N$, with $\phi_{n,i}\left(k\right)\in\{0,1\}$, $1\leq i\leq N_t$, such that $\|\boldsymbol{\phi}_n(k)\|^2=1$ and $\boldsymbol{\phi}_m^T(k)\boldsymbol{\phi}_n\left(k\right)=0$, $n\neq m$. We assume that all the subsets of the selected antennas are equally probable.

Consider the special case of $N_t=2$ and $N=1$. Denote $\mathbf{h}=[h_1\ \ h_2]^T$, $V=\max(|h_1|^2,|h_2|^2)$, and $W=\min(|h_1|^2,|h_2|^2)$. Note that in this case the received channel power at each sub-block is either $A\left(k\right)=V$ or $A\left(k\right)=W$, each of which occurs with a probability of $1/2$. Thus, given $V=v$, $W=w$, and a fixed threshold $\bar{A}\geq 0$, the amount of harvested energy in each block with BRBs is obtained using (12) as

$$E^{(\mathrm{B})}\left(v,w,\bar{A}\right)=\begin{cases}P\left(v+w\right)/2 & , \quad \bar{A}<w\\ Pv/2 & , \quad w\leq\bar{A}\leq v\\ 0 & , \quad \bar{A}>v.\end{cases} \tag{29}$$

Similar to TS-U, in the i.i.d. fading MISO channel, it can be shown that with $N_t=2$ and $N=1$ the unconditional distribution of $A\left(k\right)$ with BRBs after averaging over the fading channels is the exponential distribution, where the unconditional PDF is also given by $q_A^{(\mathrm{B})}\left(a\right)=e^{-a}$. Therefore, given a fixed threshold $\bar{A}\geq 0$, $\bar{E}^{(\mathrm{B})}\left(\bar{A}\right)=\bar{E}^{(\mathrm{U})}\left(\bar{A}\right)$ and $\bar{R}^{(\mathrm{B})}\left(\bar{A}\right)=\bar{R}^{(\mathrm{U})}\left(\bar{A}\right)$, where $\bar{E}^{(\mathrm{B})}\left(\bar{A}\right)$ and $\bar{R}^{(\mathrm{B})}\left(\bar{A}\right)$ denote the average harvested energy and achievable average information rate for TS with BRBs (referred to as TS-B), respectively, and $\bar{E}^{(\mathrm{U})}\left(\bar{A}\right)$ and $\bar{R}^{(\mathrm{U})}\left(\bar{A}\right)$ for TS-U are given by (26) and (27), respectively. In addition, given fixed $\bar{A}\geq 0$ and per-block energy harvesting requirement $\hat{E}>0$, the energy outage probability of TS-B in the i.i.d. Rayleigh fading MISO channel with $N_t=2$ and $N=1$ can be obtained from (29) as (see Appendix H for the detailed derivation)

$$\begin{aligned}p_{E,out}^{(\mathrm{B})}=&\left(1-e^{-\bar{A}}\right)^2+\mathbf{1}\left(\bar{A}<2D\right)\cdot 2e^{-2\left(\bar{A}+D\right)}\left(-1+e^{\bar{A}}\right)\left(-e^{\bar{A}}+e^{2D}\right)\\&+\mathbf{1}\left(\bar{A}<D\right)\left(e^{-2\left(\bar{A}+D\right)}\left(e^{\bar{A}}-e^{D}\right)^2+e^{-\bar{A}-2D}\left(\left(-1+\bar{A}-D\right)e^{\bar{A}}+e^{D}\right)\right),\end{aligned} \tag{30}$$

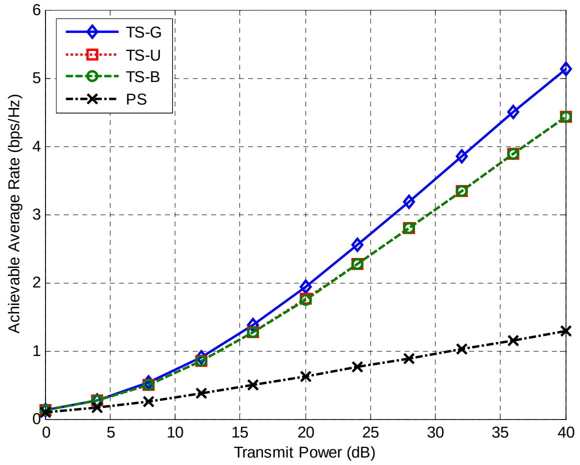

Fig. 14. Comparison of the achievable average rate for different RB designs with $N_t = 2$, $N = 1$, and the average harvested energy requirement $\bar{E} = 0.9$.

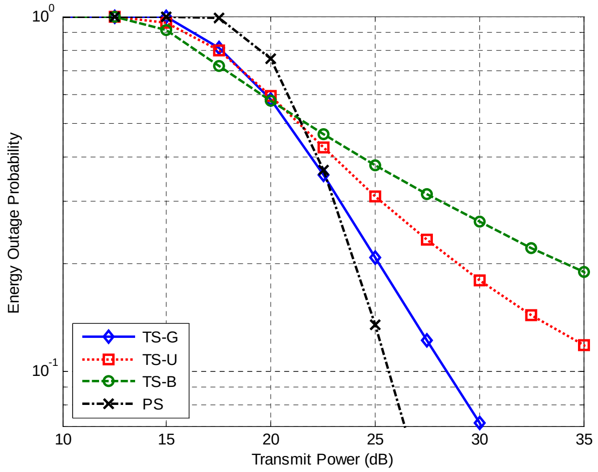

Fig. 15. Comparison of energy outage probability for different RB designs with $N_t = 2$, $N = 1$, $\bar{R} = 4$ bps/Hz, and $\hat{E} = 50$.

where $D = \frac{\hat{E}}{P}$, and $\mathbf{1}(x < y)$ denotes the indicator function given by

$$\mathbf{1}(x < y) = \begin{cases} 1 & , \text{ if } x < y \\ 0 & , \text{ otherwise.} \end{cases}$$

From (30), it is shown that both $\mathbf{1}\left(\bar{A} < 2D\right) = 0$ and $\mathbf{1}\left(\bar{A} < D\right) = 0$ if $P > 2\hat{E}/\bar{A}$, and thus $p^{(\mathrm{B})}_{E,out} = (1 - e^{-\bar{A}})^2$. Therefore, TS-B in the case of $N_t = 2$ and $N = 1$ also has the energy diversity order of 0, the same as TS-G and TS-U.

Fig. 14 shows the achievable average rates for TS-G, TS-U, TS-B, and PS versus P for a given average harvested energy (normalized by P), $\bar{E} = 0.9$. It is observed that the achievable average information rates of TS-U and TS-B are the same, which is as expected for the considered case here of $N_t = 2$ and $N = 1$. It is also observed that the achievable average rates of TS-U and TS-B are larger than that of PS, but smaller than that of TS-G. This result is originated from the fact that the artificial channel fading generated by URBs or BRBs in this case is less substantial over time than that by GRBs, due to the limitation of constant average transmit power over sub-blocks with URBs or BRBs.

Fig. 15 shows the energy outage probabilities of TS-U and TS-B versus P when $\bar{R} = 4$ bps/Hz and $\hat{E} = 50$, as compared to that of PS and TS-G. Among TS schemes, it is observed that the energy outage probability of TS-B is the smallest when P is small, i.e., $P < 20$dB, while that of TS-G is the smallest when $P \geq 20$dB. The energy outage probability of TS-U is observed to be between that of TS-B and of TS-G. It is also observed that the energy outage probability of PS is larger than that of TS schemes when P is small, but is the smallest when $P > 22.5$dB.

V. CONCLUSION

This paper studied a novel receiver mode switching scheme for the point-to-point MISO SWIPT system when the fading channel is only perfectly known at the receiver, but unknown at the transmitter. The proposed scheme exploits the benefit of opportunistic energy harvesting over artificial channel fading induced by employing multi-antenna random beamforming at the transmitter. By investigating the achievable average information rate, average harvested energy/energy outage probability, and their various trade-offs, it is revealed that the proposed scheme yields better energy and information transfer performance than the conventional periodic switching without random beamforming when the harvested energy requirement is sufficiently large. Particularly, employing one single random beam for the proposed scheme is proved to achieve the asymptotically optimal trade-off between the average information rate and average harvested energy when transmit power goes to infinity. Moreover, it is shown by simulations that the best trade-offs between average information rate and average harvested energy/energy outage probability are also achieved by the proposed scheme employing one single random beam for large energy harvesting targets of most practical interests, even with finite transmit power. Finally, it is worth noting that the results of this paper can be directly applied to the multi-user MISO multicast system for SWIPT, where multiple receivers harvest energy and decode (common) information from the signals broadcast by a single transmitter.

APPENDIX A
DERIVATIONS OF $R^{(\mathrm{T})}\left(h,1,\bar{A}\right)$ AND $R^{(\mathrm{T})}\left(h,2,\bar{A}\right)$

From (7) with $N = 1$ and (14), $R^{(\mathrm{T})}\left(h,1,\bar{A}\right)$ can be expressed as

$$R^{(\mathrm{T})}\left(h,1,\bar{A}\right) = \frac{1}{\ln 2}\int_0^{\bar{A}} \ln\left(1+Pa\right)\frac{1}{h}e^{-\frac{a}{h}}da \tag{31}$$

$$= \frac{1}{\ln 2}\left(e^{-\frac{\bar{A}}{h}}\ln\left(1+P\bar{A}\right) + \int_0^{\bar{A}}\frac{P}{1+Pa}e^{-\frac{a}{h}}da\right), \tag{32}$$

where (32) is obtained from integrating (31) by part. By changing a variable as $x = 1 + Pa$, the integral term in (32) can be obtained as

$$\begin{aligned}\int_0^{\bar{A}} \frac{P}{1+Pa} e^{-\frac{a}{h}} da &= \int_1^{1+P\bar{A}} \frac{1}{x} e^{-\frac{x-1}{Ph}} dx \\ &= e^{-\frac{1}{Ph}} \left(\int_1^{\infty} \frac{1}{x} e^{-\frac{x}{Ph}} dx - \int_{1+P\bar{A}}^{\infty} \frac{1}{x} e^{-\frac{x}{Ph}} dx \right) \quad (33) \\ &= e^{-\frac{1}{Ph}} \left(E_1\left(\frac{1}{Ph}\right) - E_1\left(\frac{1+P\bar{A}}{Ph}\right) \right), \quad (34)\end{aligned}$$

where, for integer $n \geq 0$, $E_n(z) = \int_1^{\infty} e^{-zt} t^{-n} dt$ denotes the exponential integral function; (34) is obtained by a change of variable as $y = \left(1 + P\bar{A}\right) x$ for the second integral term in (33). From (32) and (34), $R^{(\mathrm{T})}\left(h, 1, \bar{A}\right)$ is obtained as

$$R^{(\mathrm{T})}\left(h,1,\bar{A}\right) = \frac{e^{-\frac{1}{Ph}}}{\ln 2} \left(E_1\left(\frac{1}{Ph}\right) - E_1\left(\frac{1+P\bar{A}}{Ph}\right) \right) - e^{-\frac{\bar{A}}{h}} \log_2\left(1+P\bar{A}\right). \quad (35)$$

When $N = 2$, $R^{(\mathrm{T})}\left(h, 2, \bar{A}\right)$ can be derived similarly by integrating (14) by part. In this operation, it is necessary to apply differentiation of the incomplete Gamma function given by [19]

$$\frac{\partial}{\partial N} \Gamma(N, x) = \Gamma(N, x) \ln x + x G_{2,3}^{3,0}\left(\begin{array}{c} 0, 0 \\ N-1, -1, -1 \end{array} \middle| x \right), \quad (36)$$

where $G_{p,q}^{m,n}\left(\begin{array}{c} a_1, \cdots, a_p \\ b_1, \cdots, b_q \end{array} \middle| z \right)$ denotes the Meijer-G function, defined as [17, 9.301]

$$G_{p,q}^{m,n}\left(\begin{array}{c} a_1, \cdots, a_p \\ b_1, \cdots, b_q \end{array} \middle| z \right) = \frac{1}{2\pi i} \int_L \frac{\prod_{j=1}^{m} \Gamma(b_j - s) \prod_{k=1}^{n} \Gamma(1 - a_k + s)}{\prod_{j=m+1}^{q} \Gamma(1 - b_j + s) \prod_{k=n+1}^{p} \Gamma(a_k - s)} z^s ds, \quad (37)$$

with $\int_L$ denoting the Barres integral. By the definition of the Meijer-G function, the last term in (36) can be represented by

$$\begin{aligned} x G_{2,3}^{3,0}\left(\begin{array}{c} 0, 0 \\ N-1, -1, -1 \end{array} \middle| x \right) &= \frac{1}{2\pi i} \int_L \frac{\Gamma(N-1-s)\Gamma(-1-s)\Gamma(-1-s)}{\Gamma(-s)\Gamma(-s)} x^{s+1} ds \quad (38) \\ &= G_{2,3}^{3,0}\left(\begin{array}{c} 1, 1 \\ 0, 0, N \end{array} \middle| x \right), \quad (39) \end{aligned}$$

where (39) is achieved by a change of variable as $t = s + 1$ in (38). By applying (36)-(39) to the integration of (14) by part, $R^{(\mathrm{T})}\left(h, 2, \bar{A}\right)$ can be obtained as

$$\begin{aligned} R^{(\mathrm{T})}\left(h,2,\bar{A}\right) = & \left(\frac{2}{Ph} e^{-\frac{2\bar{A}}{h}} - e^{\frac{2}{Ph}} \Gamma\left(2, \frac{2\left(1+P\bar{A}\right)}{Ph}\right) \right) \log_2\left(1+P\bar{A}\right) \\ & + \frac{2}{Ph \ln 2} e^{\frac{2}{Ph}} \left(E_1\left(\frac{2\left(1+P\bar{A}\right)}{Ph}\right) - E_1\left(\frac{2}{Ph}\right) \right) \\ & + \frac{1}{\ln 2} e^{\frac{2}{Ph}} \left(G_{2,3}^{3,0}\left(\begin{array}{c} 1, 1 \\ 0, 0, 2 \end{array} \middle| \frac{2}{Ph} \right) - G_{2,3}^{3,0}\left(\begin{array}{c} 1, 1 \\ 0, 0, 2 \end{array} \middle| \frac{2\left(1+P\bar{A}\right)}{Ph} \right) \right). \quad (40) \end{aligned}$$

APPENDIX B

PROOF OF PROPOSITION 3.1

With $P \to \infty$, the achievable average information rate for TS is expressed from (17) as

$$\mathbb{E}_H\left[R^{(\mathrm{T})}\left(h, N, \bar{A}\right)\right] = \mathbb{E}_H\left[F_{A|H}^{(N)}\left(\bar{A}\,|h\right)\right]\log_2 P + \mathbb{E}_H\left[C_0\left(h, N, \bar{A}\right)\right].$$

Since $C_0\left(h, N, \bar{A}\right)$ is a constant not related to P, so is $\mathbb{E}_H\left[C_0\left(h, N, \bar{A}\right)\right]$ and thus $\mathbb{E}_H\left[C_0\left(h, N, \bar{A}\right)\right]$ is regarded as $o\left(\log_2 P\right)$.

For an integer $N \geq 1$, note that $\Gamma\left(N, x\right)$ is equivalently expressed as [15]

$$\Gamma\left(N, x\right) = \left(N-1\right)!\, e^{-x} \sum_{m=0}^{N-1} \frac{x^m}{m!}. \tag{41}$$

From (8), (15), and (41), $F_A^{(N)}\left(a\right) = \mathbb{E}_H\left[F_{A|H}^{(N)}\left(a\,|h\right)\right]$ is obtained as

$$\begin{aligned} F_A^{(N)}\left(a\right) &= \int_0^\infty F_{A|H}^{(N)}\left(a\,|h\right) f_H\left(h\right) dh \\ &= \int_0^\infty \left(1 - e^{-\frac{Na}{h}} \sum_{m=0}^{N-1} \frac{1}{m!}\left(\frac{Na}{h}\right)^m\right) \frac{N_t^{N_t}}{\Gamma\left(N_t\right)} h^{N_t-1} e^{-N_t h} dh \\ &= 1 - \frac{N_t^{N_t}}{\Gamma\left(N_t\right)} \sum_{m=0}^{N-1} \frac{1}{m!}\left(Na\right)^m \underbrace{\int_0^\infty h^{N_t-m-1} e^{-N_t h - \frac{Na}{h}} dh}_{\triangleq\, \alpha}. \end{aligned} \tag{42}$$

By applying [17, 3.471-9] to α, we can obtain (19). This completes the proof of Proposition 3.1.

APPENDIX C

PROOF OF PROPOSITION 3.2

From (13), (15), and (41), $\bar{E}^{(\mathrm{T})}\left(N, \bar{A}\right) = \mathbb{E}_H\left[E^{(\mathrm{T})}\left(h, N, \bar{A}\right)\right]$ is further obtained as

$$\begin{aligned} \bar{E}^{(\mathrm{T})}\left(N, \bar{A}\right) &= P\mathbb{E}_H\left[h e^{-\frac{N\bar{A}}{h}} \sum_{k=0}^{N} \frac{1}{k!}\left(N\bar{A}\right)^k h^{-k}\right] \\ &= P\mathbb{E}_H\left[e^{-\frac{N\bar{A}}{h}} \sum_{k=0}^{N} \frac{1}{k!}\left(N\bar{A}\right)^k h^{1-k}\right] \\ &= P\frac{N_t^{N_t}}{\Gamma\left(N_t\right)} \sum_{k=0}^{N} \frac{1}{k!}\left(N\bar{A}\right)^k \underbrace{\int_0^\infty h^{N_t-k} e^{-N_t h - \frac{N\bar{A}}{h}} dh}_{\triangleq\, \beta}. \end{aligned} \tag{43}$$

By applying [17, 3.471-9] to β in (43), we obtain (21). This completes the proof of Proposition 3.2.

APPENDIX D
PROOF OF THEOREM 3.1

First, the former part of Theorem 3.1 can be proved using the following lemma by considering an arbitrary distribution of A with PDF and CDF denoted by $g_A(a)$ and $G_A(a)$, respectively, where $G_A(a) > 0$ for $a > 0$.

Lemma D.1: Given $G_A\left(\bar{A}\right) = \tau$ with $0 < \tau < 1$ and $0 < \bar{A} < \infty$,

$$\int_{\bar{A}}^{\infty} a g_A(a)\, da > (1-\tau)\, b. \tag{44}$$

Proof: Please refer to Appendix E. ■

For TS, we have the rate scaling factor $\Delta^{(\mathrm{T})}\left(N, \bar{A}\right) = F_A^{(N)}\left(\bar{A}\right)$ from Proposition 3.1, and it can be shown from (19) that $F_A^{(N)}(a) > 0$ for $a > 0$. In addition, the energy scaling factor for TS can be alternatively expressed as $\Pi^{(\mathrm{T})}\left(N, \bar{A}\right) = \int_{\bar{A}}^{\infty} a f_A^{(N)}(a) da$ with $f_A^{(N)}(a) = \mathbb{E}_H\left[f_{A|H}^{(N)}(a\,|h)\right]$ denoting the unconditional PDF of A after averaging over the fading distribution. Furthermore, it can be easily verified that $\int_0^{\infty} a f_A^{(N)}(a) da = 1$. Given $F_A^{(N)}\left(\bar{A}\right) = \tau$ with $0 < \bar{A} < \infty$ and $0 < \tau < 1$, it can thus be verified from Lemma D.1 that $\Delta^{(\mathrm{T})}\left(N, \bar{A}\right) + \Pi^{(\mathrm{T})}\left(N, \bar{A}\right) > 1$, by substituting b, $g_A(a)$, and $G_A(a)$ in Lemma D.1 by 1, $f_A^{(N)}(a)$, and $F_A^{(N)}(a)$, respectively. Since we have $\Delta^{(\mathrm{P})}(\tau) + \Pi^{(\mathrm{P})}(\tau) = 1$ for PS from (20) and (22), it follows that $\Delta^{(\mathrm{T})}\left(N, \bar{A}\right) + \Pi^{(\mathrm{T})}\left(N, \bar{A}\right) > \Delta^{(\mathrm{P})}(\tau) + \Pi^{(\mathrm{P})}(\tau)$. Therefore, we have $\Delta^{(\mathrm{T})}\left(N, \bar{A}\right) > \Delta^{(\mathrm{P})}(\tau)$ for given $0 < \Pi^{(\mathrm{T})}\left(N, \bar{A}\right) = \Pi^{(\mathrm{P})}(\tau) < 1$. This proves the former part of Theorem 3.1.

It is worth remarking that Lemma D.1 implies that TS in general yields better trade-off between the rate and energy scaling factors than PS provided that the average received channel power for TS is the same as that for PS, based on which the former part of Theorem 3.1 for the i.i.d. Rayleigh fading MISO channel with a fixed threshold $\bar{A}$ is proved. As another example, even for a transmission block with $H = h$, TS with N RBs, $1 \leq N \leq N_t$, yields better trade-off between the rate and energy scaling factors than PS. This can be proved by substituting b, $g_A(a)$, and $G_A(a)$ in Lemma D.1 by h, $f_{A|H}^{(N)}(\bar{A}\,|h)$ in (7), and $F_{A|H}^{(N)}(\bar{A}\,|h)$ in (8), respectively. This is originated from the fact that for both TS and PS schemes the rate scaling factor is determined by the percentage of sub-blocks allocated to ID mode, whereas the energy scaling factor is determined by the percentage of sub-blocks assigned to EH mode as well as their channel power values. Note that TS scheme assigns a subset of sub-blocks with the largest channel power to EH mode, as inferred from (6). Therefore, given a percentage of sub-blocks allocated to EH mode, i.e., $1 - G_A\left(\bar{A}\right) = 1 - \tau$ for TS and PS schemes, respectively, the energy scaling factor of TS is larger than that of PS while rate scaling factors are the same for both schemes, i.e., $G_A\left(\bar{A}\right) = \tau$.

Next, to prove the latter part of Theorem 3.1, we consider two arbitrary distributions of A with PDFs denoted by $g_A(a)$ and $u_A(a)$, and the corresponding CDFs denoted by $G_A(a)$ and $U_A(a)$, respectively. It is assumed that

$\int_0^\infty a g_A(a)\, da = \int_0^\infty a u_A(a)\, da = b > 0$. It is further assumed that $G_A(a) > 0$ and $U_A(a) > 0$ for $a > 0$, and $G_A(a)$ and $U_A(a)$ intersect at $a = \hat{A}$, satisfying

$$\begin{cases} G_A(a) > U_A(a), & \text{if } 0 < a < \hat{A} \\ G_A(a) = U_A(a), & \text{if } a = \hat{A} \\ G_A(a) < U_A(a), & \text{if } a > \hat{A}. \end{cases} \tag{45}$$

Lemma D.2: Given $0 < G_A\left(\bar{A}_g\right) = U_A\left(\bar{A}_u\right) < 1$ with $0 < \bar{A}_g, \bar{A}_u < \infty$,

$$\int_{\bar{A}_g}^{\infty} a g_A(a)\, da > \int_{\bar{A}_u}^{\infty} a u_A(a)\, da. \tag{46}$$

Proof: Please refer to Appendix F. ■

The latter part of Theorem 3.1 can be proved using Lemma D.2 as follows. Given $1 \le N < M \le N_t$ for TS, it can be verified that $\int_0^\infty a f_A^{(N)}(a)\, da = \int_0^\infty a f_A^{(M)}(a)\, da = 1$. Furthermore, it can be shown from (19) that $F_A^{(N)}(a)$ and $F_A^{(M)}(a)$ correspond to $G_A(a)$ and $U_A(a)$ in (45), respectively (c.f. Fig. 8). By substituting $f_A^{(N)}(a)$, $f_A^{(M)}(a)$, $F_A^{(N)}(a)$, and $F_A^{(M)}(a)$ for $g_A(a)$, $u_A(a)$, $G_A(a)$, and $U_A(a)$ in Lemma D.1, respectively, it can be verified that $\Pi^{(\mathrm{T})}\left(N, \bar{A}_N\right) > \Pi^{(\mathrm{T})}\left(M, \bar{A}_M\right)$ when $\Delta^{(\mathrm{T})}\left(N, \bar{A}_N\right) = \Delta^{(\mathrm{T})}\left(M, \bar{A}_M\right)$, $0 < \bar{A}_N, \bar{A}_M < \infty$ since $\Delta^{(\mathrm{T})}\left(N, \bar{A}_N\right) = F_A^{(N)}(a)$ from Proposition 3.1 and $\Pi^{(\mathrm{T})}\left(N, \bar{A}_N\right) = \int_{\bar{A}_N}^\infty a f_A^{(N)}(a) da$. This guarantees that $\Delta^{(\mathrm{T})}\left(N, \bar{A}_N\right) > \Delta^{(\mathrm{T})}\left(M, \bar{A}_M\right)$ for given $0 < \Pi^{(\mathrm{T})}\left(N, \bar{A}_N\right) = \Pi^{(\mathrm{T})}\left(M, \bar{A}_M\right) < 1$, since both $\Delta^{(\mathrm{T})}\left(N, \bar{A}_N\right)$ and $\Delta^{(\mathrm{T})}\left(M, \bar{A}_M\right)$ decrease monotonically with increasing $\Pi^{(\mathrm{T})}\left(N, \bar{A}_N\right)$ and $\Pi^{(\mathrm{T})}\left(M, \bar{A}_M\right)$, respectively. This proves the latter part of Theorem 3.1.

As a remark, Lemma D.2 compares the trade-offs between the rate and energy scaling factors in TS schemes with two different distributions of channel power induced by different values of N provided that both distributions have the same average channel power and satisfy the condition in (45). The latter part of Theorem 3.1 for the i.i.d Rayleigh fading MISO channel with a fixed $\bar{A}$ is one application of Lemma D.2. As another example, even for a transmission block with $H = h$, better trade-off between the rate and energy scaling factors is attained with N than M RBs, $1 \le N < M \le N_t$, since $F_{A|H}^{(N)}(a\,|h)$ and $F_{A|H}^{(M)}(a\,|h)$ correspond to $G_A(a)$ and $U_A(a)$ in (45), respectively, as shown from (8). This is due to the fact that the artificial channel fading is more substantial when smaller number of RBs is employed, and the argument similarly as for Lemma D.1.

Combining the proofs for both the above two parts, Theorem 3.1 is proved.

APPENDIX E
PROOF OF LEMMA D.1

Integrating by part, $\int_0^{\bar{A}} a g_A(a)\, da$ can be evaluated as

$$\int_0^{\bar{A}} a g_A(a)\, da = \bar{A} G_A\left(\bar{A}\right) - \int_0^{\bar{A}} G_A(a)\, da. \tag{47}$$

Assume that $\bar{A}$ is given such that $G_A\left(\bar{A}\right) = \tau$, $0 < \tau < 1$. From (44) and (47), we have

$$\begin{aligned}\tilde{E} &= \int_{\bar{A}}^{\infty} a g_A\left(a\right) da - \left(1 - \tau\right) b \\ &= \int_{0}^{\infty} a g_A\left(a\right) da - \int_{0}^{\bar{A}} a g_A\left(a\right) da - b\left(1 - G_A\left(\bar{A}\right)\right) \\ &= \left(b - \bar{A}\right) G_A\left(\bar{A}\right) + \int_{0}^{\bar{A}} G_A\left(\bar{A}\right) da, \qquad (48)\end{aligned}$$

and the resulting derivative

$$\mu = \frac{d\tilde{E}}{d\bar{A}} = \left(b - \bar{A}\right) g_A\left(\bar{A}\right), \qquad (49)$$

where $\mu = 0$ is achieved at $\bar{A} = b$.

From (48) and (49), it is observed that $\tilde{E} > 0$ with $0 < \bar{A} \leq b$, and $\tilde{E}$ increases monotonically with $\bar{A}$ until $\bar{A} = b$. For $\bar{A} > b$, it is observed that $\mu < 0$ and thus $\tilde{E}$ decreases monotonically with increasing $\bar{A}$. Because $\lim_{\bar{A} \to \infty} \int_{\bar{A}}^{\infty} a g_A\left(a\right) da = 0$, it can be shown that $\tilde{E} > 0$ even with $\bar{A} > b$. Therefore, it is verified that $\tilde{E} > 0$ in (48) for any $\bar{A} > 0$. This completes the proof of Lemma D.1.

APPENDIX F
PROOF OF LEMMA D.2

Denote $\Delta = G_A(\bar{A}_g) = U_A(\bar{A}_u)$, $0 < \bar{A}_g, \bar{A}_u < \infty$. From (46) and (47), we have

$$\begin{aligned}\tilde{E} &= \int_{\bar{A}_g}^{\infty} a g_A\left(a\right) da - \int_{\bar{A}_u}^{\infty} a u_A\left(a\right) da \\ &= \int_{0}^{\bar{A}_u} a u_A\left(a\right) da - \int_{0}^{\bar{A}_g} a g_A\left(a\right) da \qquad (50) \\ &= \Delta\left(\bar{A}_u - \bar{A}_g\right) + \int_{0}^{\bar{A}_g} G_A\left(a\right) da - \int_{0}^{\bar{A}_u} U_A\left(a\right) da. \qquad (51)\end{aligned}$$

According to (45), there are three cases addressed as follows for given $0 < \Delta < 1$.

1) $\bar{A}_g = \bar{A}_u = \hat{A}$: According to (45), $G_A(\hat{A}) = U_A(\hat{A}) = \hat{\Delta}$. Since it is assumed in (45) that $G_A(a) > U_A(a)$ with $0 < a < \hat{A}$, $\tilde{E}$ is evaluated from (51) as

$$\tilde{E} = \int_{0}^{\hat{A}} \left(G_A\left(a\right) - U_A\left(a\right)\right) da > 0. \qquad (52)$$

2) $0 < \bar{A}_g, \bar{A}_u < \hat{A}$: It can be inferred from (45) that $\bar{A}_g < \bar{A}_u < \hat{A}$, which results in $0 < \Delta < \hat{\Delta}$. From (51), we have

$$\tilde{E} = \underbrace{U_A\left(\bar{A}_u\right)\left(\bar{A}_u - \bar{A}_g\right) - \int_{\bar{A}_g}^{\bar{A}_u} U_A\left(a\right) da}_{\triangleq\, \beta} + \underbrace{\int_{0}^{\bar{A}_g} \left(G_A\left(a\right) - U_A\left(a\right)\right) da}_{\triangleq\, \alpha}. \qquad (53)$$

Since $\bar{A}_g < \bar{A}_u$ and $G_A(a) > U_A(a)$ with $0 < a < \hat{A}$, it can be verified that $\alpha > 0$ and $\beta > 0$, and thus $\tilde{E} > 0$.

3) $\hat{A} < \bar{A}_g, \bar{A}_u < \infty$: It can be inferred from (45) that $\hat{A} < \bar{A}_u < \bar{A}_g$, which results in $\hat{\Delta} < \Delta < 1$. From (50), we have

$$\tilde{E} = \underbrace{\int_0^{\hat{A}} a\left(u_A\left(a\right) - g_A\left(a\right)\right) da}_{\triangleq\, \delta} - \underbrace{\left(\int_{\hat{A}}^{\bar{A}_g} a g_A\left(a\right) da - \int_{\hat{A}}^{\bar{A}_u} a u_A\left(a\right) da\right)}_{\triangleq\, \varepsilon}, \tag{54}$$

with $\delta > 0$ as shown in (50)-(52). In addition, it can be verified that

$$\lim_{\Delta \to \hat{\Delta}} \varepsilon = \lim_{\bar{A}_g \to \hat{A}} \int_{\hat{A}}^{\bar{A}_g} a g_A\left(a\right) da - \lim_{\bar{A}_u \to \hat{A}} \int_{\hat{A}}^{\bar{A}_u} a u_A\left(a\right) da = 0, \tag{55}$$

$$\lim_{\Delta \to 1} \varepsilon = \lim_{\substack{\bar{A}_g \to \infty, \\ \bar{A}_u \to \infty}} \varepsilon = \int_0^{\hat{A}} a u_A\left(a\right) da - \int_0^{\hat{A}} a g_A\left(a\right) da = \delta. \tag{56}$$

Since $\frac{d\Delta}{d\bar{A}_g} = \frac{d}{d\bar{A}_g} G_A\left(\bar{A}_g\right) = g_A\left(\bar{A}_g\right)$ and $\frac{d\Delta}{d\bar{A}_u} = \frac{d}{d\bar{A}_u} U_A\left(\bar{A}_u\right) = u_A\left(\bar{A}_u\right)$, we have

$$\begin{aligned} \frac{d}{d\Delta}\varepsilon &= \frac{1}{\frac{d\Delta}{d\bar{A}_g}} \frac{d}{d\bar{A}_g} \int_{\hat{A}}^{\bar{A}_g} a g_A\left(a\right) da - \frac{1}{\frac{d\Delta}{d\bar{A}_u}} \frac{d}{d\bar{A}_u} \int_{\hat{A}}^{\bar{A}_u} a u_A\left(a\right) da \\ &= \bar{A}_g - \bar{A}_u > 0. \end{aligned} \tag{57}$$

From (54)-(57), it can be verified that $\tilde{E}$ monotonically decreases from δ to 0 with increasing Δ with $\hat{\Delta} < \Delta < 1$, i.e., $\tilde{E} > 0$ with $\hat{A} < \bar{A}_g, \bar{A}_u < \infty$.

Combining the above three cases, Lemma D.2 is thus proved.

APPENDIX G

PROOF OF PROPOSITION 3.3

Given a transmission block with $H = h$, $E^{(\mathrm{T})}\left(h, N, 0\right) = Ph$ from (13). In the i.i.d. Rayleigh fading MISO channel, given $\hat{E} > 0$, $p_{E,out}^{(\mathrm{T})}$ for TS with $\bar{A} = 0$ can be approximated as $P \to \infty$ by $\lim\limits_{P \to \infty} \Pr\left(h < \frac{\hat{E}}{P}\right) = \lim\limits_{P \to \infty} F_H\left(\frac{\hat{E}}{P}\right) = \left(\frac{\hat{E}}{P}\right)^{N_t}$, since $\lim\limits_{h \to 0} F_H\left(h\right) = h^{N_t}$ in (16). This proves the first equality in (24) for $\bar{A} = 0$.

When $\bar{A} > 0$, the harvested energy per block for a given h, $E^{(\mathrm{T})}\left(h, N, \bar{A}\right)$ in (13), is a monotonically increasing function of h, since $\Gamma\left(\alpha, x\right)$ is a monotonically decreasing function of x. For a given energy requirement $\hat{E} > 0$, denote $\bar{h}$ as the minimum value of h such that $E^{(\mathrm{T})}\left(\bar{h}, N, \bar{A}\right) \geq \hat{E}$, i.e.,

$$\theta\left(\bar{h}\right) \triangleq \bar{h}\, \frac{\Gamma\left(N+1, N\bar{A}/\bar{h}\right)}{\Gamma\left(N+1\right)} = \frac{\hat{E}}{P}. \tag{58}$$

Thus, the energy outage probability for TS with given N, $\bar{A}$, and $\hat{E}$ is obtained as $p_{E,out}^{(\mathrm{T})}(N, \bar{A}, \hat{E}) = F_H(\bar{h})$.

Since $\theta\left(h\right)$ increases with h, with $P \to \infty$ it then follows from (58) that $\bar{h} \to 0$, under which we have

$$\theta\left(\bar{h}\right) = \bar{h}e^{-\left(N\bar{A}/\bar{h}\right)}\sum_{k=0}^{N}\frac{1}{k!}\left(\frac{N\bar{A}}{\bar{h}}\right)^{k} \tag{59}$$

$$\approx \bar{h}e^{-\left(N\bar{A}/\bar{h}\right)}\frac{1}{N!}\left(\frac{N\bar{A}}{\bar{h}}\right)^{N}, \tag{60}$$

where (59) is obtained from (41) since $N \geq 1$ is an integer. Since $\ln\theta\left(\bar{h}\right) = \ln\frac{\hat{E}}{P}$, from (60), we have

$$(N-1)\ln x - N\bar{A}x = \ln\left(\frac{\hat{E}N!}{P\left(N\bar{A}\right)^{N}}\right), \tag{61}$$

where $x = 1/\bar{h}$. With $\bar{h} \to 0$, i.e., $x \to \infty$, the left-hand side of (61) can be further approximated as $-N\bar{A}x$. Therefore, $\bar{h}$ as $P \to \infty$ can be approximated by

$$\bar{h} = N\bar{A}\left(\ln\left(\frac{P\left(N\bar{A}\right)^{N}}{\hat{E}N!}\right)\right)^{-1} \approx N\bar{A}(\ln P)^{-1}. \tag{62}$$

From (62) and the fact that $F_H\left(h\right) \approx h^{N_t}$ as $h \to 0$, we obtain the second equality in (24) for $\bar{A} > 0$.

From the proofs for both the first and second equalities in (24), Proposition 3.3 is thus proved.

APPENDIX H

DERIVATION OF (30)

From (29), the energy outage probability of TS-B is obtained as

$$p_{E,out}^{(\mathrm{B})} = \Pr\left(v < \bar{A}\right) + \Pr\left(w \leq \bar{A} \leq v,\ \frac{Pv}{2} < \hat{E}\right) + \Pr\left(w > \bar{A},\ \frac{P\left(v+w\right)}{2} < \hat{E}\right). \tag{63}$$

First, $\Pr\left(v < \bar{A}\right)$ in (63) is given by

$$\Pr\left(v < \bar{A}\right) = F_V\left(\bar{A}\right) = \left(1 - e^{-\bar{A}}\right)^2, \tag{64}$$

where $F_V\left(v\right)$ denotes the CDF of $V = \max(\left|h_1\right|^2, \left|h_2\right|^2)$, given by $F_V\left(v\right) = (1 - e^{-v})^2$, since both $\left|h_1\right|^2$ and $\left|h_2\right|^2$ are independent exponential random variables.

The second term in (63) can be obtained as

$$\begin{aligned}\Pr\left(w \leq \bar{A} \leq v,\ \frac{Pv}{2} < \hat{E}\right) &= \Pr\left(w \leq \bar{A},\ \bar{A} \leq v \leq 2D,\ w \leq v\right)\\ &= \mathbf{1}\left(\bar{A} < 2D\right)\int_{\bar{A}}^{2D}\int_{0}^{\bar{A}} f_{V,W}\left(v,w\right)dwdv\\ &= \mathbf{1}\left(\bar{A} < 2D\right)2e^{-2\left(\bar{A}+D\right)}\left(-1+e^{\bar{A}}\right)\left(-e^{\bar{A}}+e^{2B}\right), \end{aligned} \tag{65}$$

where $D = \frac{\hat{E}}{P}$ and $f_{V,W}\left(v,w\right)$ denotes the joint PDF for V and W given by $f_{V,W}\left(v,w\right) = 2e^{-v}e^{-w}$, $v > w$.

Finally, the last term in (63) can be obtained as

$$
\begin{aligned}
&\Pr\left(w > \bar{A},\, \frac{P\left(v+w\right)}{2} < \hat{E}\right)\\
&= \Pr\left(w > \bar{A},\, v+w < 2D\right)\\
&= \mathbf{1}\left(\bar{A} < D\right)\left(\int_{\bar{A}}^{B}\int_{\bar{A}}^{v} f_{V,W}\left(v,w\right)dwdv + \int_{B}^{2B-\bar{A}}\int_{\bar{A}}^{2B-v} f_{V,W}\left(v,w\right)dwdv\right)\\
&= \mathbf{1}\left(\bar{A} < D\right)\left(e^{-2\left(\bar{A}+D\right)}\left(e^{\bar{A}} - e^{D}\right)^{2} + e^{-\bar{A}-2D}\left(\left(-1+\bar{A}-D\right)e^{\bar{A}} + e^{D}\right)\right). \qquad (66)
\end{aligned}
$$

From (63)-(66), we can obtain (30).

REFERENCES

[1] L. R. Varshney, “Transporting information and energy simultaneously,” in *Proc. IEEE Int. Symp. Inf. Theory (ISIT)*, pp. 1612-1616, July 2008.

[2] X. Zhou, R. Zhang, and C. K. Ho, ”Wireless information and power transfer: architecture design and rate-energy trade-off,” in *Proc. IEEE Global Commun. Conf. (GLOBECOM)*, pp. 1-5, Dec. 2012.

[3] P. Grover and A. Sahai, “Shannon meets Tesla: wireless information and power transfer,” in *Proc. IEEE Int. Symp. Inf. Theory (ISIT)*, pp. 2363-2367, June 2010.

[4] L. Liu, R. Zhang, and K. C. Chua, “Wireless information transfer with opportunistic energy harvesting,” *IEEE Trans. Wireless Commun.*, accepted for publication.

[5] R. Zhang and C. K. Ho, “MIMO broadcasting for simultaneous wireless information and power transfer,” in *Proc. IEEE Global Commun. Conf. (GLOBECOM)*, pp. 1-5, Dec. 2011.

[6] Z. Xiang and M. Tao, “Robust beamforming for wireless information and power transmission,” *IEEE Wireless Commun. Letters*, vol. 1, no. 4, pp. 372-375, Aug. 2012.

[7] B. K. Chalise, Y. D. Zhang, and M. G. Amin, “Energy harvesting in an OSTBC based amlify-and-forward MIMO relay system,” in *Proc. IEEE Int. Conf. on Acousitcs, Speech, and Signal Process. (ICASSP)*, pp. 3201-3204, Mar. 2012.

[8] A. M. Fouladgar and O. Simeone, “On the transfer of information and energy in multi-user systems,” *IEEE Commun. Letters*, vol. 16, no. 11, pp. 1733-1736, Nov. 2012.

[9] I. E. Telatar, “Capacity of multi-antenna Gaussian channels,” *European Trans. Tecelcommun.*, vol. 10, pp. 585-595, Nov/Dec 1999

[10] S. M. Alamouti, “A simple transmit diversity technique for wireless communications,” *IEEE J. Sel. Areas Commun.*, vol. 16, no. 8, pp. 1277-1294, Oct. 1998.

[11] V. Tarokh, H. Jafarkhani, and A. R. Calderbank, “Space-time block code from orthogonal designs,” *IEEE Trans. Inf. Theory*, vol. 45, no. 5, pp. 1456-1467, July 1999.

[12] P. Viswanath, D. N. C. Tse, and R. Laroia, “Opportunistic beamforming using dumb antennas,” *IEEE Trans. Inf. Theory*, vol. 48, no. 6, pp. 1277-1294, June 2002

[13] M. Sharif and B. Hassibi, “On the capacity of MIMO broadcast channels with partial side information,” *IEEE Trans. Inf. Theory*, vol. 51, no. 2, pp. 506-522, Feb. 2005.

[14] D. J. C. Mackay, “Fountain codes,” *IEE Proceedings, Communications*, vol. 152, no. 6, pp. 1062-1068, Dec. 2005.

[15] J. G. Proakis, Digital Communication, 4th edition, McGraw-Hill, 2000.

[16] N. Alon, J. Edmonds, and M. Luby, “Linear time erasure codes with nearly optimal recovery,” in *Proc. the 36th IEEE Annual Symp. Foundations of Computer Science*, pp. 512-519, Oct. 1995.

[17] I. S. Gradshteyn and I. I. Ryshik, *Table of Integrals, Series, and Products*, Academia Press, sixth edition, 2000

[18] B. Hassibi and T. L. Marzetto, “Multiple-antennas and isotropically random unitary inputs: the received signal density in closed form,” *IEEE Trans. Inf. Theory*, vol. 48, no. 6, pp. 1473-1484, June 2002.

[19] K. O. Geddes, M. L. Glasser, R. A. Moore, and T. C. Scott, “Evaluation of classes of definite integrals involving elementary functions via differentiation of special functions, Applicable Algebra in Engineering, Communication and Computing (AAECC), vol. 1, pp. 149-165, 1990.